

Electronic Supplementary Information

The first hydride–Meisenheimer adduct of electron-deficient 3-nitronaphthalimide: Application to colorimetric borohydride determination

Myung Gil Choi, Na Yeong Kim, Yu Jeong Lee, Sangdoon Ahn* and Suk-Kyu Chang*

Department of Chemistry, Chung-Ang University, Seoul 06974, Republic of Korea

Experimental Procedures.

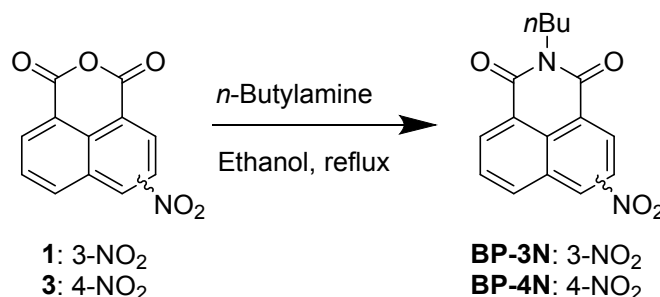
- Table S1.** Overview of the published borohydride detection methods
- Table S2.** Calculated thermochemistry values of the formation of the hydride–Meisenheimer adducts
- Scheme S1.** Resonance structures of the hydride–Meisenheimer adducts derived from **BP-3N** and **BP-4N**.
- Fig. S1.** Effect of pH on the borohydride signaling of **BP-3N** as monitored by the changes in absorbance at 523 nm.
- Fig. S2.** UV–vis spectra of several electron deficient naphthalimides (**BP-3N**, **BP-3B**, **BP-4N**, and **BP-4B**) and corresponding anhydride precursors (**1–4**) in the presence and absence of borohydride in 100% DMSO.
- Fig. S3.** Time-dependent absorbance changes at 523 nm for **BP-3N** upon treatment with borohydride.
- Fig. S4.** HSQC and HMBC spectra of hydride–Meisenheimer adduct **5** in DMSO-*d*₆.
- Fig. S5.** HSQC and HMBC spectra of deuteride–Meisenheimer adduct **6** in DMSO-*d*₆.
- Fig. S6.** Partial ¹³C NMR spectra of **BP-3N** and **BP-3N** in the presence of BH₄[−] (**BP-3N** + NaBH₄).
- Fig. S7.** High-resolution ESI mass spectrum of hydride–Meisenheimer adduct **5** obtained from **BP-3N** after treatment with sodium borohydride in acetonitrile.
- Fig. S8.** ¹H and ¹³C NMR spectra of deuteride–Meisenheimer adduct **6** in DMSO-*d*₆.

- Fig. S9.** High-resolution ESI mass spectrum of deuteride-Meisenheimer adduct **6** obtained from **BP-3N** after treatment with NaBD₄.
- Fig. S10.** UV-vis spectra of **BP-4N** in the presence and absence of borohydride in aqueous DMSO.
- Fig. S11.** Optimized structures of **BP-3N**, 2-positioned-, and 4-positioned-Meisenheimer adducts.
- Fig. S12.** Fluorescence spectra of **BP-3N** in the presence and absence of borohydride, and *n*-butyl-4-aminonaphthalimide (4-NH₂-NPI) as the fluorescence reference.
- Fig. S13.** Selective borohydride signaling of **BP-3N** over common anions as expressed by the absorbance ratio (A/A_0) at 523 nm.
- Fig. S14.** Selective borohydride signaling of **BP-3N** over common reactive oxygen and nitrogen species (ROS/RNS) as expressed by the absorbance ratio (A/A_0) at 523 nm.
- Fig. S15.** The time-course plot of the absorbance change of **BP-3N** at 523 nm during reaction with borohydride.
- Fig. S16.** Concentration dependence of borohydride signaling by **BP-3N**.
- Fig. S17.** ¹H NMR spectrum of **BP-3N** in DMSO-*d*₆ (600 MHz).
- Fig. S18.** ¹³C NMR spectrum of **BP-3N** in DMSO-*d*₆ (150 MHz).
- Fig. S19.** Electron ionization mass spectrum (direct insertion probe) of **BP-3N**.
- Fig. S20.** ¹H NMR spectrum of **BP-3B** in DMSO-*d*₆ (600 MHz).
- Fig. S21.** ¹³C NMR spectrum of **BP-3B** in DMSO-*d*₆ (150 MHz).
- Fig. S22.** Electron ionization mass spectrum (direct insertion probe) of **BP-3B**.
- Fig. S23.** ¹H NMR spectrum of **BP-4N** in DMSO-*d*₆ (600 MHz).
- Fig. S24.** ¹³C NMR spectrum of **BP-4N** in DMSO-*d*₆ (150 MHz).
- Fig. S25.** Electron ionization mass spectrum (direct insertion probe) of **BP-4N**.
- Fig. S26.** ¹H NMR spectrum of **BP-4B** in DMSO-*d*₆ (600 MHz).
- Fig. S27.** ¹³C NMR spectrum of **BP-4B** in DMSO-*d*₆ (150 MHz).
- Fig. S28.** Electron ionization mass spectrum (direct insertion probe) of **BP-4B**.
- Fig. S29.** ¹H NMR spectrum of hydride-Meisenheimer adduct **5** in DMSO-*d*₆ (600 MHz).
- Fig. S30.** ¹³C NMR spectrum of hydride-Meisenheimer adduct **5** in DMSO-*d*₆ (150 MHz).

Experimental Procedures

General. Sodium borohydride, sodium borodeuteride (NaBD₄), 3-nitro-1,8-naphthalic anhydride (**1**), 3-bromo-1,8-naphthalic anhydride (**2**), 4-nitro-1,8-naphthalic anhydride (**3**), 4-bromo-1,8-naphthalic anhydride (**4**), *n*-butylamine, metal perchlorates, and the sodium salts of anions were purchased from Sigma-Aldrich. Sodium borohydride was used after standardization via iodometry.^{S1} ¹H and ¹³C NMR spectra were measured at 600 and 150 MHz, respectively, on a Varian VNS NMR spectrometer. UV-vis and fluorescence spectra were recorded on a Scinco S-3100 spectrophotometer and Scinco FS-2 fluorescence spectrophotometer, respectively. High-resolution mass spectrometry data were recorded using a Bruker Compact mass spectrometer with electrospray ionization (ESI). Low-resolution mass spectrometry results were obtained using a Micromass Autospec mass spectrometer with electron ionization (EI). Column chromatography was carried out using silica gel (240 mesh, Merck).

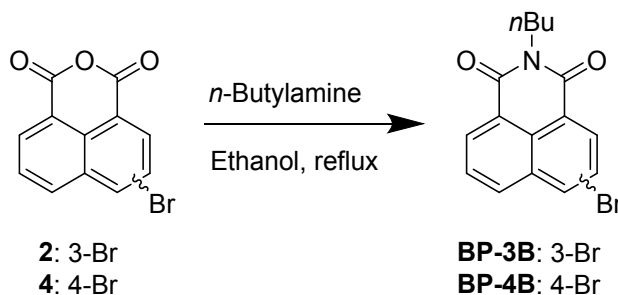
Preparation of *n*-butyl-nitro-1,8-naphthalimide derivatives (BP-3N and BP-4N). 3-Nitro-1,8-naphthalic anhydride (**1**) (0.26 g, 1.0 mmol) or 4-nitro-1,8-naphthalic anhydride (**3**) (0.26 g, 1.0 mmol) was dissolved in 20 mL of ethanol. After addition of *n*-butylamine (0.198 mL, 2.0 mmol), the reaction mixture was refluxed for 12 h. After cooling the reaction mixture in an ice bath, the solvent was removed under reduced pressure. The residue was dissolved in dichloromethane, and the solution was washed with distilled water and brine. The product was obtained after purification by column chromatography using dichloromethane as the eluent.



BP-3N: White solid, 0.25 g, yield: 85%. m.p. 98°C (Lit. 97.5–98°C).^{S2} ¹H NMR (600 MHz, DMSO-*d*₆): δ 9.37 (d, *J* = 2.3 Hz, 1H), 8.83 (d, *J* = 2.3 Hz, 1H), 8.68 (dd, *J* = 8.2, 0.6 Hz, 1H), 8.58 (dd, *J* = 7.3, 1.2 Hz, 1H), 7.98 (dd, *J* = 8.2, 7.3 Hz, 1H), 3.98 (t, *J* = 7.5 Hz, 2H), 1.59 (p, *J* = 7.5 Hz, 2H), 1.34 (h, *J* = 7.4 Hz, 2H), 0.91 (t, *J* = 7.4 Hz, 3H); ¹³C NMR (150 MHz, DMSO-*d*₆): δ 163.1, 162.5, 146.1, 136.6, 134.3, 131.2, 130.0, 129.8, 129.6, 124.3, 123.2, 122.9, 40.2, 29.9, 20.2, 14.1; MS (EI) for C₁₆H₁₄N₂O₄: *m/z* calcd. 298.1, found 298.0.

BP-4N: White solid, 0.27 g, yield: 91%. m.p. 103°C (Lit. 103.5–104.5°C).^{S3} ¹H NMR (600 MHz, DMSO-*d*₆): δ 8.61 (dd, *J* = 8.6, 1.1 Hz, 1H), 8.53 (dd, *J* = 7.3, 1.1 Hz, 1H), 8.52–8.46 (m, 2H), 8.01 (dd, *J* = 8.7, 7.3 Hz, 1H), 4.00 (t, *J* = 7.4 Hz, 2H), 1.60 (p, *J* = 7.5 Hz, 2H), 1.35 (h, *J* = 7.4 Hz, 2H), 0.92 (t, *J* = 7.4 Hz, 3H); ¹³C NMR (150 MHz, DMSO-*d*₆): δ 163.2, 162.4, 149.4, 132.0, 130.5, 130.0, 129.1, 128.6, 126.9, 124.6, 123.1, 123.0, 40.2, 29.9, 20.2, 14.1; MS (EI) for C₁₆H₁₄N₂O₄: *m/z* calcd. 298.1, found 298.0.

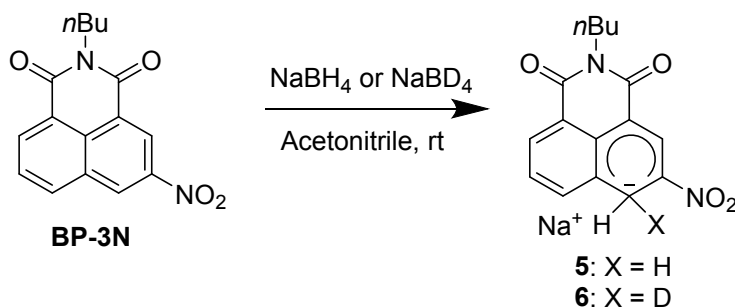
Preparation of *n*-butyl-bromo-1,8-naphthalimide derivatives (BP-3B and BP-4B). 3-Bromo-1,8-naphthalic anhydride (**2**) (0.28 g, 1.0 mmol) or 4-bromo-1,8-naphthalic anhydride (**4**) (0.28 g, 1.0 mmol) was dissolved in 20 mL of methanol. *n*-Butylamine (0.148 mL, 1.5 mmol) was added to the solution, and the reaction mixture was refluxed for 12 h. After cooling the reaction mixture in an ice bath, the solvent was removed under reduced pressure. The residue was dissolved in dichloromethane, and the solution was successively washed with distilled water and brine. The product was obtained after purification by column chromatography using dichloromethane as the eluent.



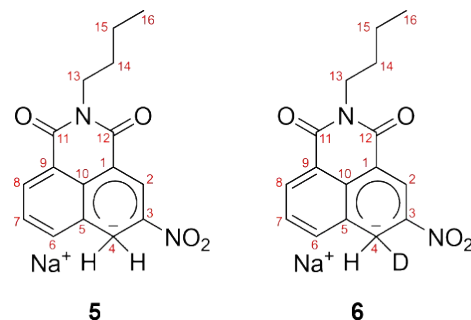
BP-3B: White solid, 0.29 g, yield: 87%. m.p. 145°C (Lit. 146–148°C).^{S4} ¹H NMR (600 MHz, DMSO-*d*₆): δ 8.65 (s, 1H), 8.41 (dd, *J* = 7.2, 1.3 Hz, 1H), 8.36 – 8.30 (m, 2H), 7.85 (t, *J* = 7.7 Hz, 1H), 3.98 (t, *J* = 7.4 Hz, 2H), 1.58 (p, *J* = 7.6 Hz, 2H), 1.34 (h, *J* = 7.4 Hz, 2H), 0.92 (t, *J* = 7.4 Hz, 3H); ¹³C NMR (150 MHz, DMSO-*d*₆): δ 163.3, 162.7, 136.1, 133.7, 133.0, 132.8, 131.4, 128.8, 126.3, 124.4, 122.6, 120.4, 40.1, 30.0, 20.2, 14.1; MS (EI) for C₁₆H₁₄BrNO₂: *m/z* calcd. 331.0, found 331.1.

BP-4B: White solid, 0.27 g, yield: 83%. m.p. 104°C (Lit. 103.5–104.5°C).^{S5} ¹H NMR (600 MHz, DMSO-*d*₆): δ 8.42 (d, *J* = 7.3 Hz, 1H), 8.37 (d, *J* = 8.5 Hz, 1H), 8.18 (d, *J* = 7.8 Hz, 1H), 8.08 (d, *J* = 7.8 Hz, 1H), 7.87 (dd, *J* = 8.5, 7.3 Hz, 1H), 3.96 (t, *J* = 7.5 Hz, 2H), 1.58 (p, *J* = 7.5 Hz, 2H), 1.34 (h, *J* = 7.4 Hz, 2H), 0.92 (t, *J* = 7.4 Hz, 3H); ¹³C NMR (150 MHz, DMSO-*d*₆): δ 163.11, 163.06, 132.8, 131.8, 131.6, 131.2, 130.0, 129.4, 129.1, 128.5, 123.0, 122.2, 39.9, 30.0, 20.2, 14.1; MS (EI) for C₁₆H₁₄BrNO₂: *m/z* calcd. 331.0, found 331.1.

Preparation of Meisenheimer adducts 5 and 6. *n*-Butyl-3-nitro-1,8-naphthalimide **BP-3N** (0.30 g, 1.0 mmol) was dissolved in 5 mL of acetonitrile. Sodium borohydride (0.042 g, 1.1 mmol) or sodium borodeuteride (0.046 g, 1.1 mmol) was added into the solution. The reaction mixture was stirred at room temperature for 30 min, and the mixture was slowly poured into 100 mL of diethyl ether. The resulting scarlet-colored precipitate was filtered and dried in a vacuum oven (40 °C).



5: Scarlet-colored solid, 0.21 g, yield: 65%. m.p. > 136°C (decomposed). ¹H NMR (600 MHz, DMSO-*d*₆): δ 8.21 (s, 1H, H-2), 7.72 (dd, *J* = 8.0, 1.4 Hz, 1H, H-8), 7.32 (dd, *J* = 7.3, 1.4 Hz, 1H, H-6), 7.03 (t, *J* = 7.6 Hz, 1H, H-7), 4.12 (s, 2H, H-4), 3.91 (t, *J* = 7.4 Hz, 2H, H-13), 1.50 (p, *J* = 7.4 Hz, 2H, H-14), 1.29 (h, *J* = 7.4 Hz, 2H, H-15), 0.90 (t, *J* = 7.4 Hz, 3H, H-16); ¹³C NMR (150 MHz, DMSO-*d*₆): δ 164.2 (C-11), 162.3 (C-12), 134.3 (C-2), 133.5 (C-9), 132.7 (C-6), 131.0 (C-10), 125.9 (C-8), 123.9 (C-7), 122.7 (C-3), 119.5 (C-5), 99.9 (C-1), 39.1 (C-13), 30.9 (C-4), 30.4 (C-14), 20.3 (C-15), 14.2 (C-16); HRMS (ESI⁻) for C₁₆H₁₅N₂O₄⁻: *m/z* calcd. 299.1037, found 299.1033.



6: Scarlet-colored solid, 0.20 g, yield: 62%. m.p. > 138°C (decomposed). ¹H NMR (600 MHz, DMSO-*d*₆): δ 8.23 (s, 1H, H-2), 7.73 (d, *J* = 7.9 Hz, 1H, H-8), 7.32 (d, *J* = 7.4 Hz, 1H, H-6), 7.04 (t, *J* = 7.6 Hz, 1H, H-7), 4.10 (s, 1H, H-4), 3.91 (t, *J* = 7.4 Hz, 2H, H-13), 1.50 (p, *J* = 7.4 Hz, 2H, H-14), 1.28 (h, *J* = 7.4 Hz, 2H, H-15), 0.89 (t, *J* = 7.4 Hz, 3H, H-16); ¹³C NMR (150 MHz, DMSO-*d*₆): δ 164.2 (C-11), 162.3 (C-12), 134.4 (C-2), 133.5 (C-9), 132.7 (C-6), 131.0 (C-10), 125.9 (C-8), 124.0 (C-7), 122.6 (C-3), 119.5 (C-5), 100.2 (C-1), 39.1 (C-13), 30.6 (t, *J*_{C-D} = 66 Hz, C-4), 30.4 (C-14), 20.3 (C-15), 14.2 (C-16); HRMS (ESI⁻) for C₁₆H₁₄DN₂O₄⁻: *m/z* calcd. 300.1100, found 300.1102.

Preparation of Na₂HPO₄-NaOH buffer solution. Na₂HPO₄-NaOH buffer solution (pH 11.0) was prepared by following the reported literature.^{S6} A solution of Na₂HPO₄ (0.20 M, 50 mL) was prepared in distilled water, and NaOH solution (0.20 M, 8.2 mL) was added into this solution. The resulting solution was diluted to 100 mL with distilled water.

Preparation of stock solutions. Stock solutions of naphthalimide compounds (**BP-3N**, **BP-3B**, **BP-4N**, and **BP-4B**) and their corresponding anhydride precursors (**1-4**) (5.0×10^{-4} M) were prepared in spectroscopy-grade DMSO. A stock solution of sodium borohydride (1.0×10^{-2} M) was made in 5 mM NaOH solution to ensure its stability. Stock solutions of metal ions (Li⁺, Na⁺, K⁺, Mg²⁺, Ca²⁺, Ba²⁺, Mn²⁺, Fe²⁺, Fe³⁺, Co²⁺, Ni²⁺, Cu²⁺, Ag⁺, Zn²⁺, Cd²⁺, Hg²⁺, Pb²⁺, and Al³⁺ as perchlorate salts) and anions (F⁻, Cl⁻, Br⁻, I⁻, HPO₄²⁻, P₂O₇⁴⁻, SO₄²⁻, NO₃⁻, N₃⁻, CO₃²⁻, OAc⁻, ClO₄⁻, and S²⁻ as sodium salts) were prepared in distilled water.

Colorimetric borohydride signaling behavior of BP-3N. All the measurements were carried out in a 55:45 (v/v) mixture of Na₂HPO₄-NaOH buffer (pH 11.0) and DMSO. Sample solutions for the determination of borohydride were prepared by mixing **BP-3N** (120 μL, 5.0×10^{-4} M), sodium borohydride (120 μL, 1.0×10^{-2} M), and Na₂HPO₄-NaOH buffer solution (300 μL, pH 11.0, 0.10 M) in a vial, and subsequently diluting with distilled water and DMSO to make a measuring solution (3.0 mL). The final concentrations of **BP-3N**, borohydride, metal ions or anions, and buffer were 2.0×10^{-5} , 4.0×10^{-4} , 4.0×10^{-4} , and 1.0×10^{-2} M, respectively. Since the stock solution of sodium

borohydride was prepared in an NaOH solution, the final NaOH concentration of all the sample solutions was equally adjusted to 1.0×10^{-3} M.

Calculation of heats of reaction of the hydride-Meisenheimer adduct. Computational calculations were performed using simplified structures of methylimide instead of *n*-butylimide to reduce the calculation time. To calculate the enthalpies of reaction ($\Delta_r H^\circ$) of the two most plausible structures of **BP-3N**, 2-positioned and 4-positioned Meisenheimer adducts, optimization of the structures of **BP-3N**, hydride, and the 2-positioned and 4-positioned Meisenheimer adducts was performed using Gaussian 09 (DFT calculation using the B3LYP method with the 6-311G++ (d,p) basis set).^{S7} The thermochemistry values, such as the sum of the electronic and zero-point energies ($\varepsilon_0 + \varepsilon_{ZPE}$), thermal energies ($\varepsilon_0 + E_{tot}$), thermal enthalpies ($\varepsilon_0 + H_{corr}$), and thermal free energies ($\varepsilon_0 + G_{corr}$), of the structures were estimated using frequency calculations in the Gaussian program. The enthalpies of reaction ($\Delta_r H^\circ$) of the Meisenheimer adducts were calculated using the equation shown below.

$$\Delta_r H^\circ = \sum (\varepsilon_0 + H_{corr})_{product} - \sum (\varepsilon_0 + H_{corr})_{reactant}$$

Quantification of borohydride in commercial reagents by BP-3N.

All measurements were conducted under an optimized condition of 55:45 (v/v) mixture of Na₂HPO₄-NaOH buffer (pH 11.0) and DMSO. All experiments were independently conducted three times.

A. Acquisition of a calibration curve for the standard borohydride. Calibration curve for the standard borohydride was obtained using a reagent standardized by iodometry.^{S1} The solutions for the construction of a calibration curve for borohydride were prepared by mixing **BP-3N** (120 μ L, 5.0×10^{-4} M), stock solutions of the standardized sodium borohydride (6.0 μ L, 12 μ L, 18 μ L, and 24 μ L, 1.0×10^{-2} M), and Na₂HPO₄-NaOH buffer solution (300 μ L, pH 11.0, 0.10 M) in a vial, and subsequently diluting with distilled water and DMSO to make measuring solutions (3.0 mL, 55:45 (v/v) mixture of buffer (final concentration = 10 mM) and DMSO). The final concentrations of **BP-3N**, standard borohydride, and buffer were 2.0×10^{-5} M, $2.0 \times 10^{-5} - 8.0 \times 10^{-5}$ M, and 1.0×10^{-2} M, respectively. The absorbance at 523 nm of the solutions was measured by a UV-vis spectrophotometer. From these results, the calibration curve for the standard borohydride was obtained, and the slope of the plot was calculated.

B. Borohydride assay of commercial reagents. To determine the borohydride assay of the commercial reagents, four solutions having different amounts of borohydride were prepared. For this, the analyte solutions were prepared by mixing **BP-3N** (120 μ L, 5.0×10^{-4} M), borohydride analyte (6.0 μ L, 12 μ L, 18 μ L, and 24 μ L, 1.0×10^{-2} M), and Na₂HPO₄-NaOH buffer solution (300 μ L, pH 11.0, 0.10 M) in a vial, and subsequently diluting with distilled water and DMSO to make final measuring solutions (3.0 mL, 55:45 (v/v) mixture of buffer (final concentration = 10 mM) and DMSO). The calibration curve was constructed by plotting the absorbance at 523 nm as a function of [borohydride], and the slope of the plot was estimated. The assay of borohydride reagent was calculated using the equation

shown below.

$$\begin{aligned} & \text{Assay of } BH_4^- \text{ reagent (\%)} \\ &= \frac{(\text{Slope of the calibration curve for the reagent})}{(\text{Slope of the calibration curve for the standard } BH_4^-)} \times 100 \% \end{aligned}$$

Table S1. Overview of the published borohydride detection methods

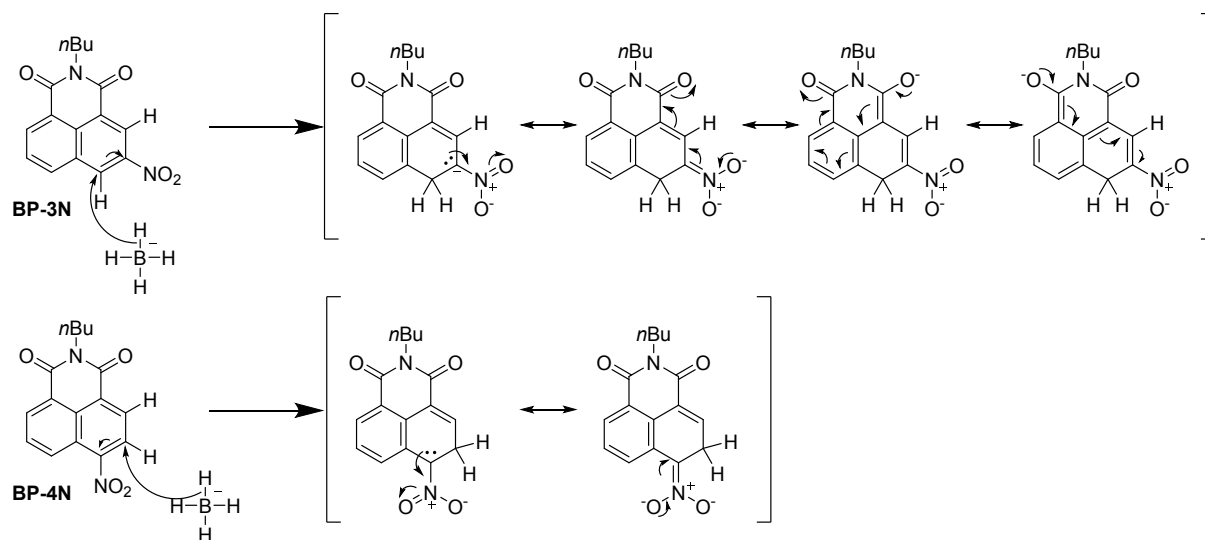
Method	Detection detail	Detection limit	Reference
Hydrogen evolution	In the presence of catalyst/Accurate	6.7×10^{-3} M (100 ppm)	S8
Hydride hydrolysis	Calibration curve needed	3.4×10^{-2} M (500 ppm)	S9
Iodate	Back-titrated with thiosulfate	1.3×10^{-3} M (20 ppm)	S1
Hypochlorite	Colorimetry , At pH range 9.6–10.3	Not reported	S10
Acetone	Reduction to isopropyl alcohol	5×10^{-5} M (0.74 ppm)	S11
Argentometry	Reaction with Ag^+ ions in the presence of ethylenediamine	2.5×10^{-5} M (0.37 ppm)	S12
Voltammetry	Using Au working electrode	3×10^{-5} M (0.44 ppm)	S13
FT-IR	Using B–H vibration frequencies	Not reported	S14
NMR	^{11}B NMR	Not reported	S15
Phosphotungstate ($\text{PW}_{12}\text{O}_{40}^{3-}$)	Colorimetry Blue-violet color at 680 nm	Spot test only	S16
Arylaldehydes (Anthracene, Pyrene)	Fluorometric analysis	7.4×10^{-6} M (0.11 ppm), 1.57×10^{-5} M (0.23 ppm),	S17
NAD ⁺ (nicotinamide adenine dinucleotide)	Colorimetry , Reduced NADH at 340 nm	6.7×10^{-5} M (1 ppm)	S18
2,4,6-Trinitrobenzene-sulfonic acid	Colorimetry , Red-orange color at 460 nm	Semiquantitative	S19
Crystal violet	Colorimetry , Suitable in non-aqueous media (DMF)	6.7×10^{-4} M 10 ppm (EtOH) Depends on matrix	S20
3-Nitronaphthalimide (BP-3N)	Colorimetry , Formation of hydride-Meisenheimer adduct	2.24×10^{-6} M (0.033 ppm)	This work

Table S2. Calculated thermochemistry values for the formation of hydride-Meisenheimer adducts

	BP-3N	Hydride	2- positioned	4- positioned
ϵ_0	-910.803146	0.438966	-911.481219	-911.495118
ϵ_{ZPE}	0.192396	0	0.201563	0.201829
E_{tot}	0.206253	0.001416	0.216543	0.216837
H_{corr}	0.207197	0.00236	0.217487	0.217782
G_{corr}	0.150873	-0.010654	0.159063	0.158876
$\epsilon_0 + \epsilon_{ZPE}$	-910.610751	-0.502257	-911.279656	-911.293289
$\epsilon_0 + E_{tot}$	-910.59689	-0.500841	-911.264675	-911.27828
$\epsilon_0 + H_{corr}$	-910.59594	-0.499897	-911.263731	-911.27733
$\epsilon_0 + G_{corr}$	-910.652273	-0.512911	-911.322156	-911.336242

- a. The structures were calculated using Gaussian 09 (DFT, B3LYP, 6-311G++ (d,p)).^{S7}
 b. Thermochemistry values such as sum of electronic and zero-point energies ($\epsilon_0 + \epsilon_{ZPE}$), thermal energies ($\epsilon_0 + E_{tot}$), thermal enthalpies ($\epsilon_0 + H_{corr}$), and thermal free energies ($\epsilon_0 + G_{corr}$) of the structures were estimated using frequency calculations.
 c. All the values are in Hartrees.

Scheme S1. Resonance structures of the hydride-Meisenheimer adducts derived from BP-3N and BP-4N.



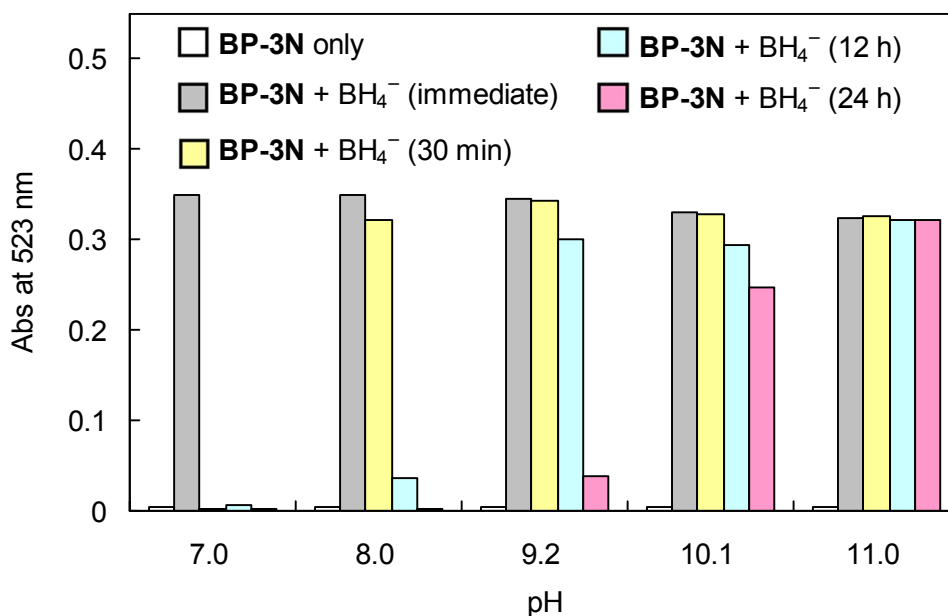


Fig. S1. Effect of pH on the borohydride signaling of **BP-3N** as monitored by the changes in absorbance at 523 nm. [**BP-3N**] = 2.0×10^{-5} M, [NaBH_4] = 4.0×10^{-4} M in 55:45 (v/v) mixture of buffer (final concentration = 10 mM) and DMSO. pH 7.0 and 8.0: phosphate buffer, pH 9.2 and 10.1: carbonate buffer, pH 11.0: $\text{Na}_2\text{HPO}_4\text{-NaOH}$ buffer. The solutions containing borohydride were incubated for a certain time (30 min – 24 h) before the addition of **BP-3N**.

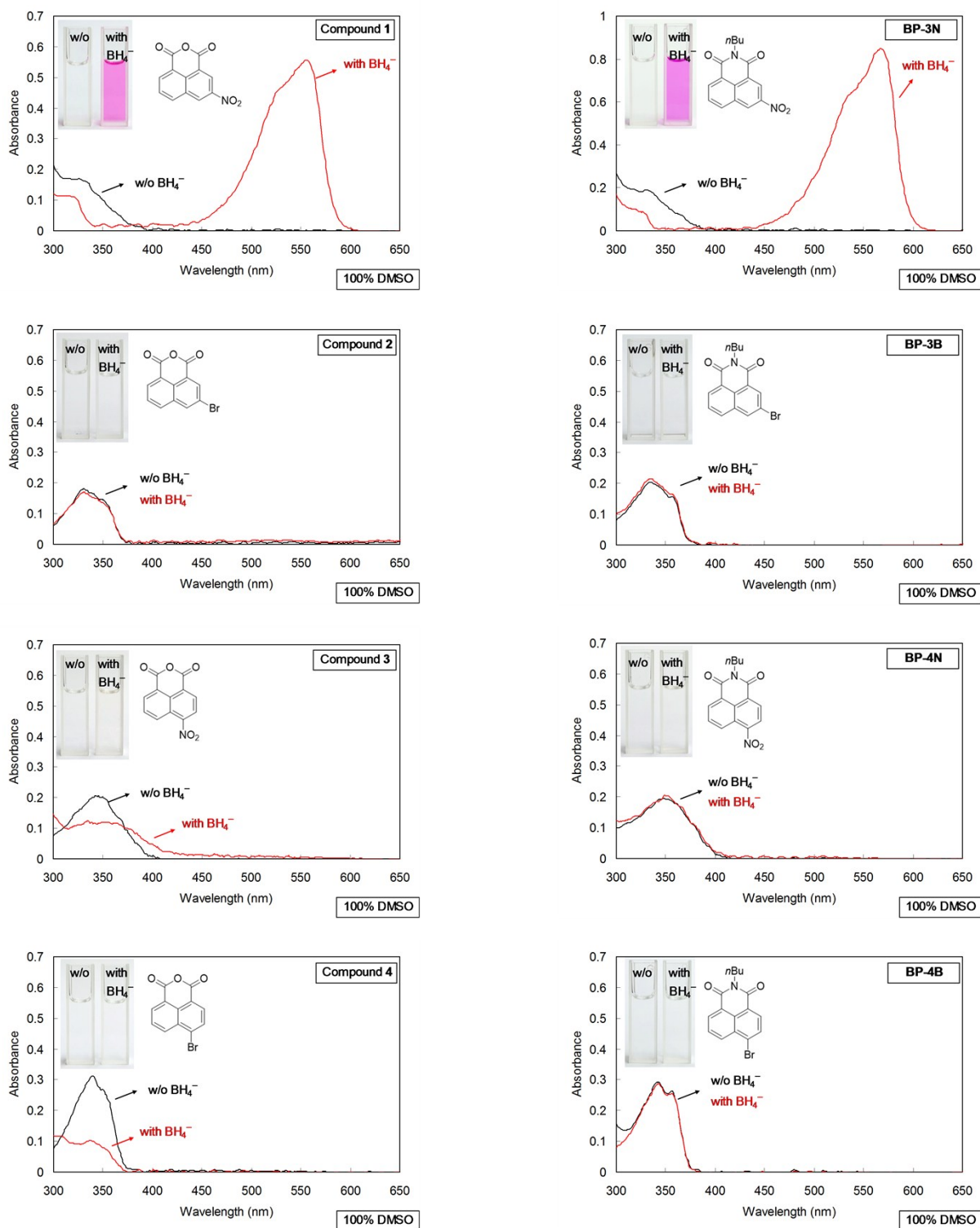


Fig. S2. UV-vis spectra of several electron-deficient naphthalimides (**BP-3N**, **BP-3B**, **BP-4N**, and **BP-4B**) and corresponding anhydride precursors (**1-4**) in the presence and absence of borohydride in 100% DMSO. [Naphthalimide] = [Naphthalic anhydride] = 2.0×10^{-5} M, $[\text{NaBH}_4] = 4.0 \times 10^{-4}$ M in DMSO.

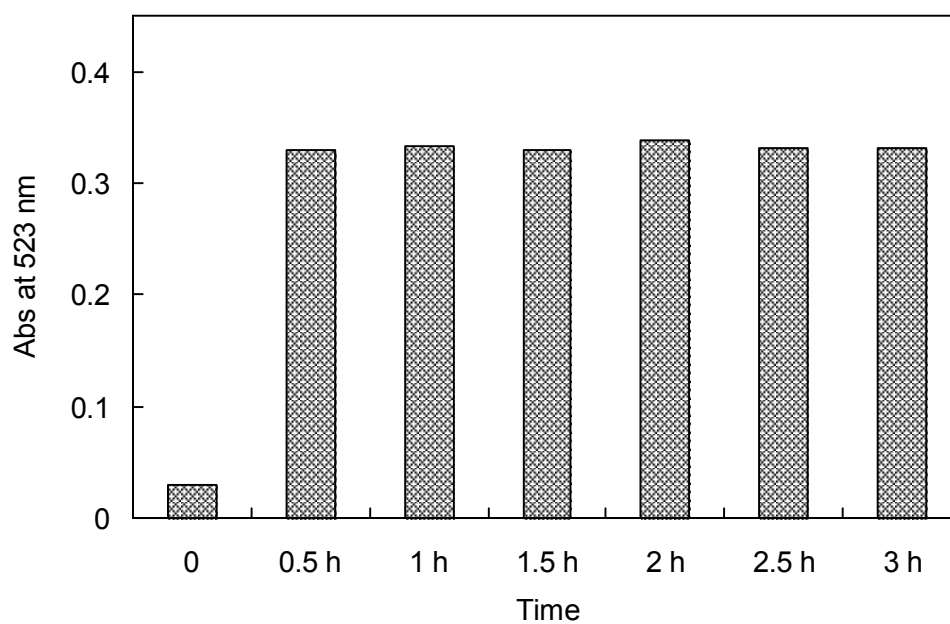
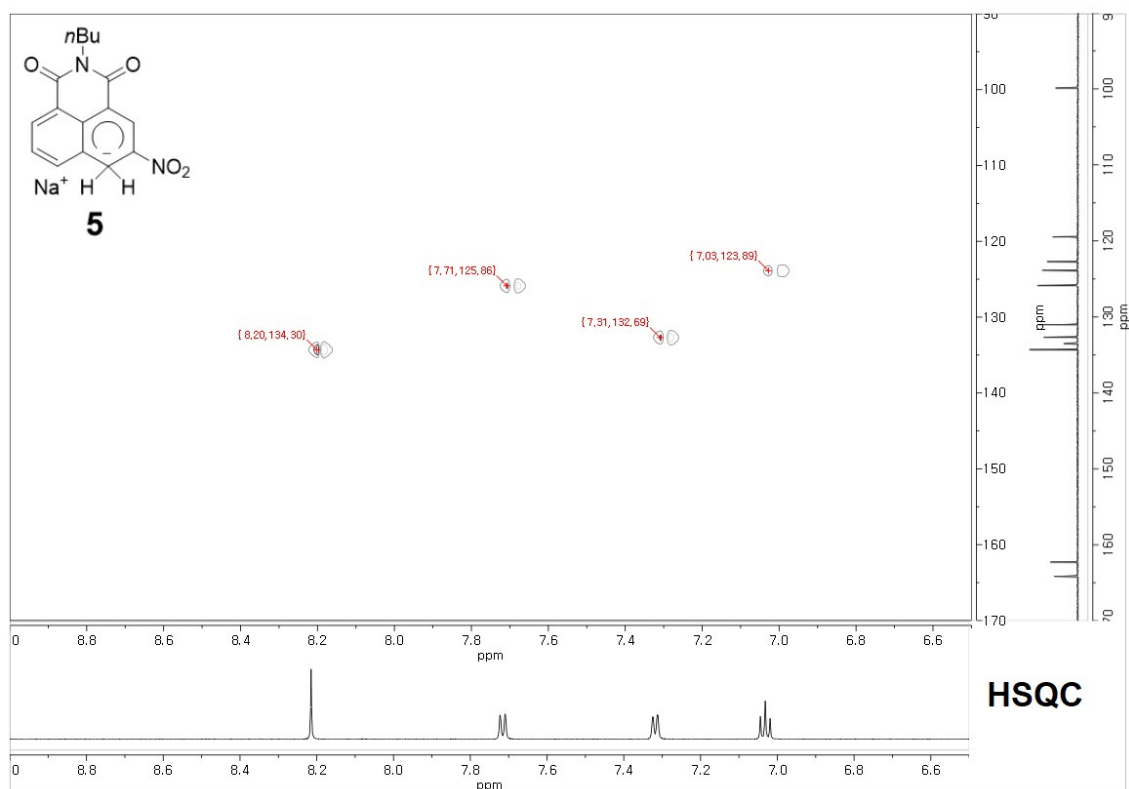


Fig. S3. Time-dependent absorbance changes at 523 nm for **BP-3N** upon treatment with borohydride. $[\text{BP-3N}] = 2.0 \times 10^{-5} \text{ M}$, $[\text{NaBH}_4] = 4.0 \times 10^{-4} \text{ M}$ in 55:45 (v/v) mixture of Na_2HPO_4 -NaOH buffer (pH 11.0, final concentration = 10 mM) and DMSO.

(a) HSQC



(b) HMBC

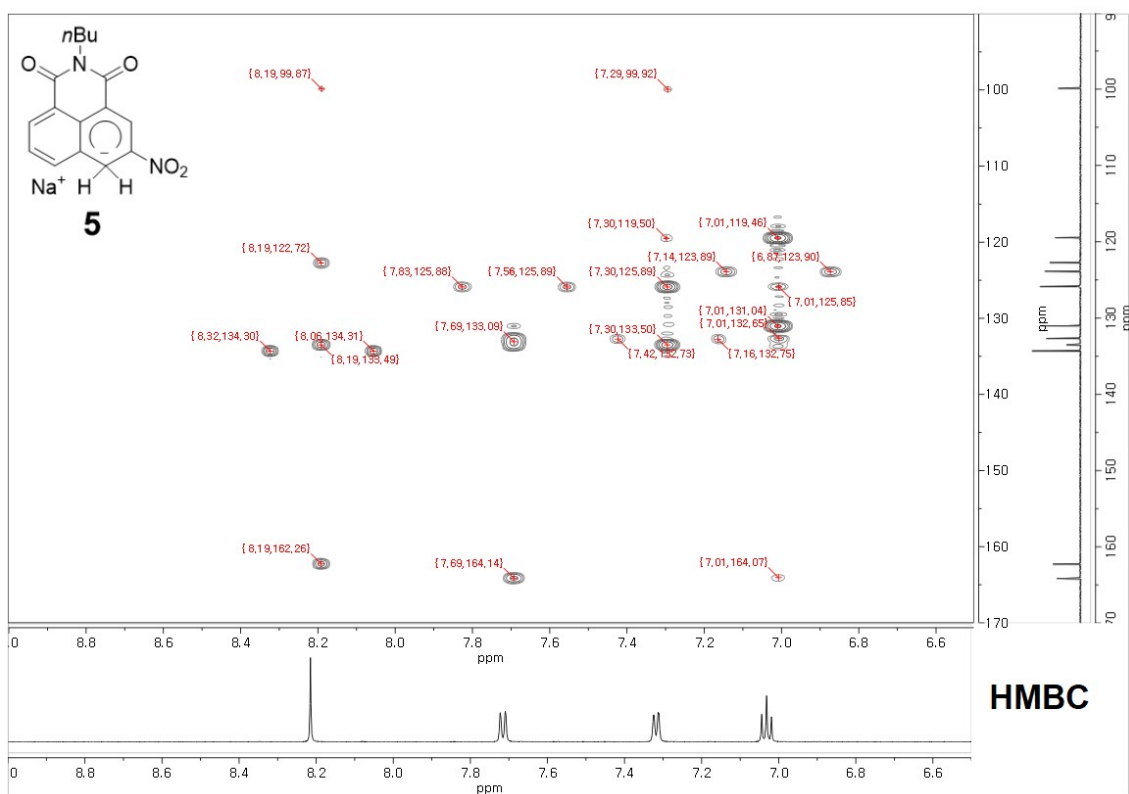
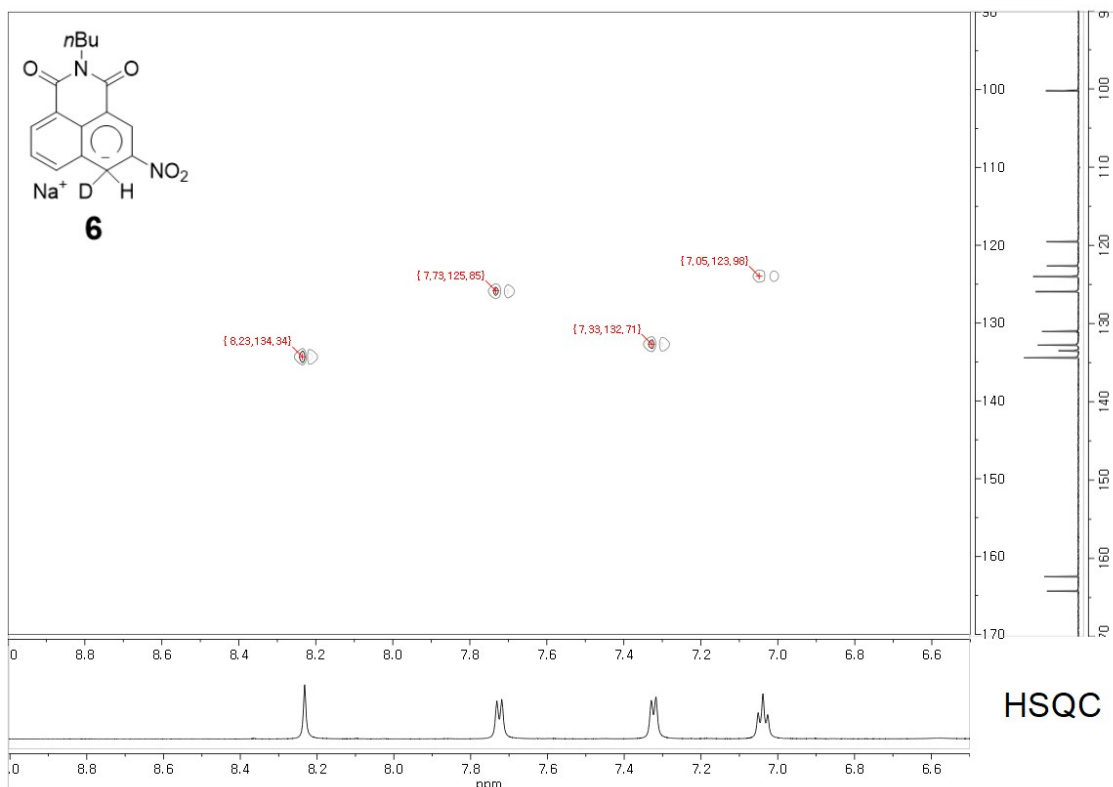


Fig. S4. HSQC and HMBC spectra of hydride-Meisenheimer adduct **5** in $\text{DMSO-}d_6$.

(a) HSQC



(b) HMBC

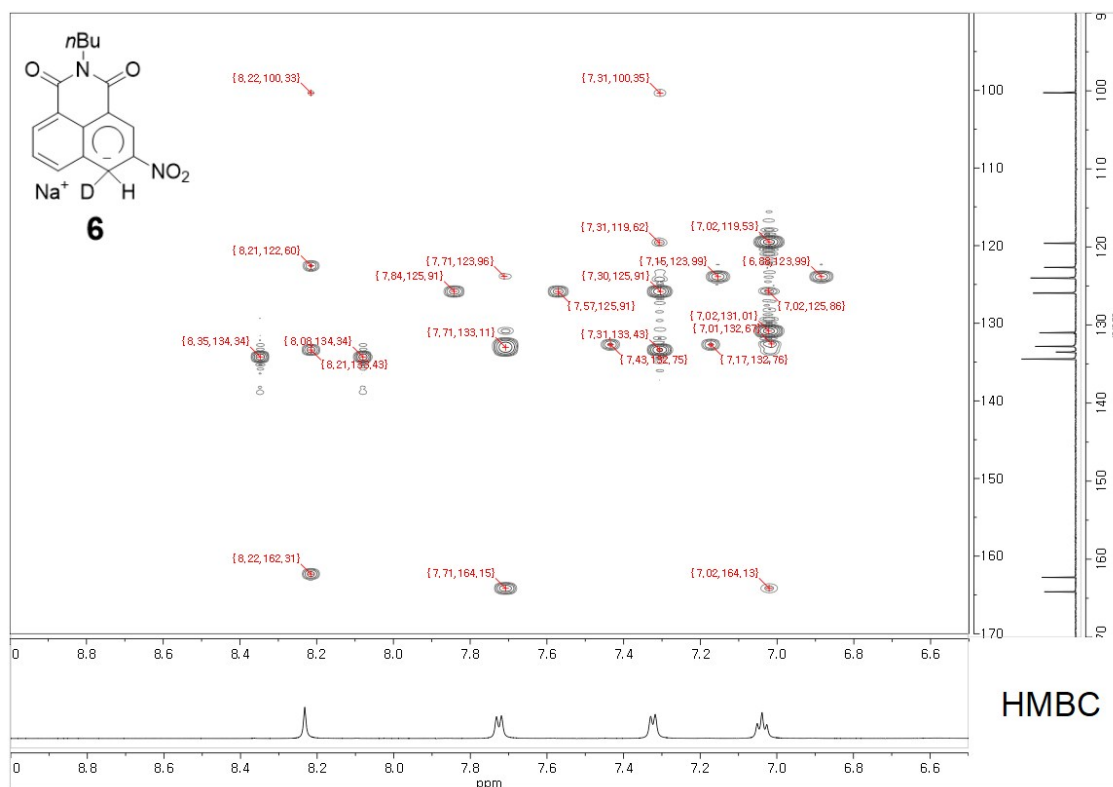


Fig. S5. HSQC and HMBC spectra of deuteride-Meisenheimer adduct **6** in $\text{DMSO-}d_6$.

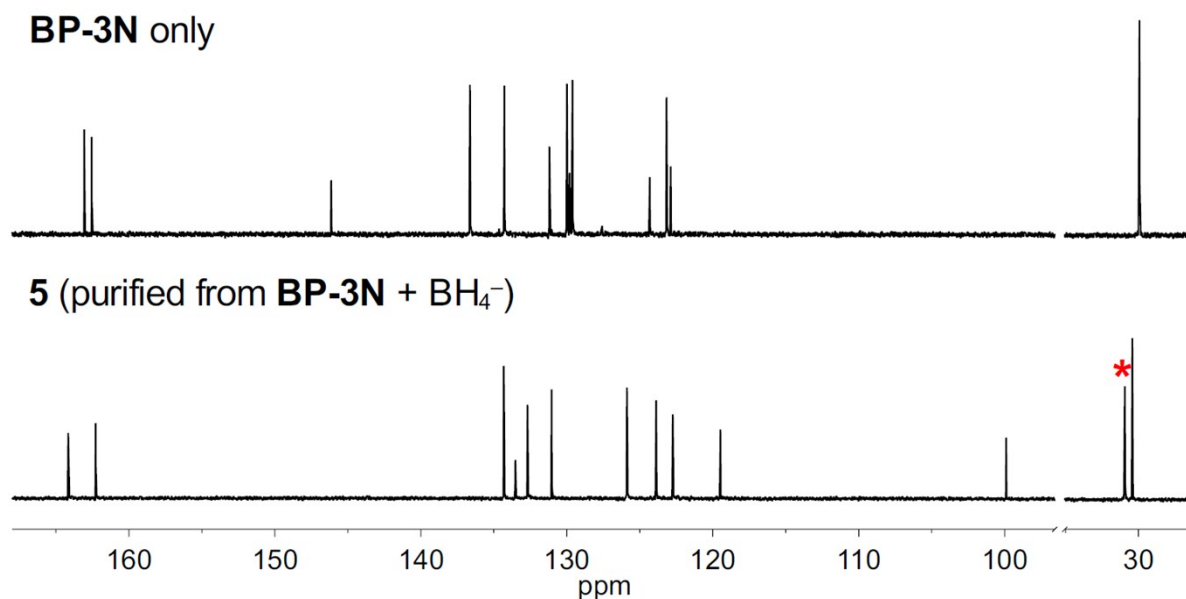


Fig. S6. Partial ¹³C NMR spectra of **BP-3N** and **BP-3N** in the presence of BH₄⁻ (**BP-3N** + NaBH₄). [**BP-3N**] = 1.0 × 10⁻² M, [**5**] = 1.0 × 10⁻² M in DMSO-*d*₆. ¹³C NMR spectrum of hydride-Meisenheimer adduct **5** (purified from **BP-3N** + BH₄⁻) was measured for a signaling product obtained by precipitation. The resonance marked with a red asterisk is due to the *sp*³ carbon (C-4) of hydride-Meisenheimer adduct **5**.

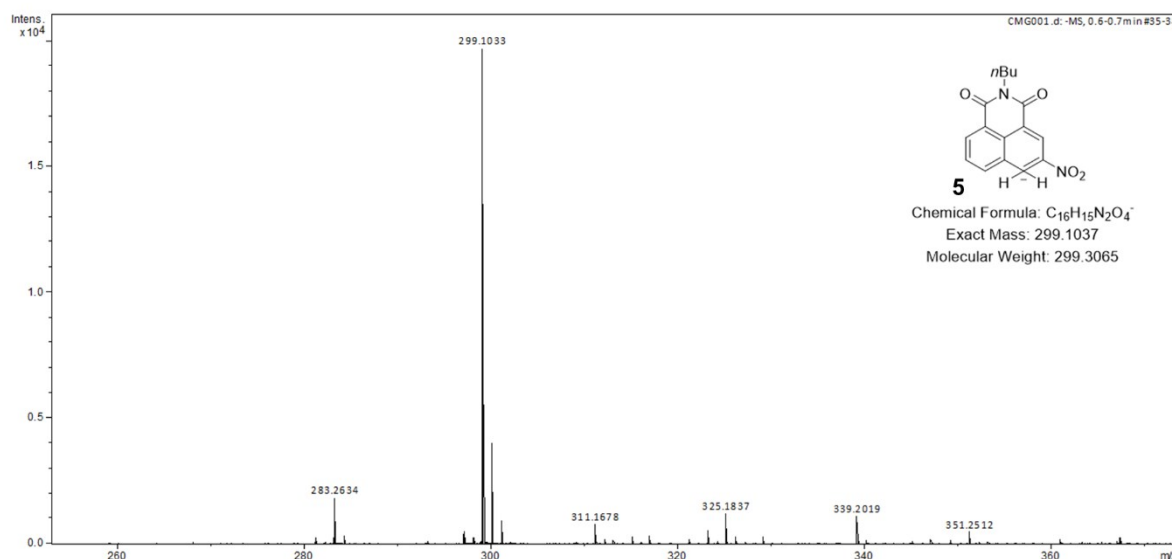
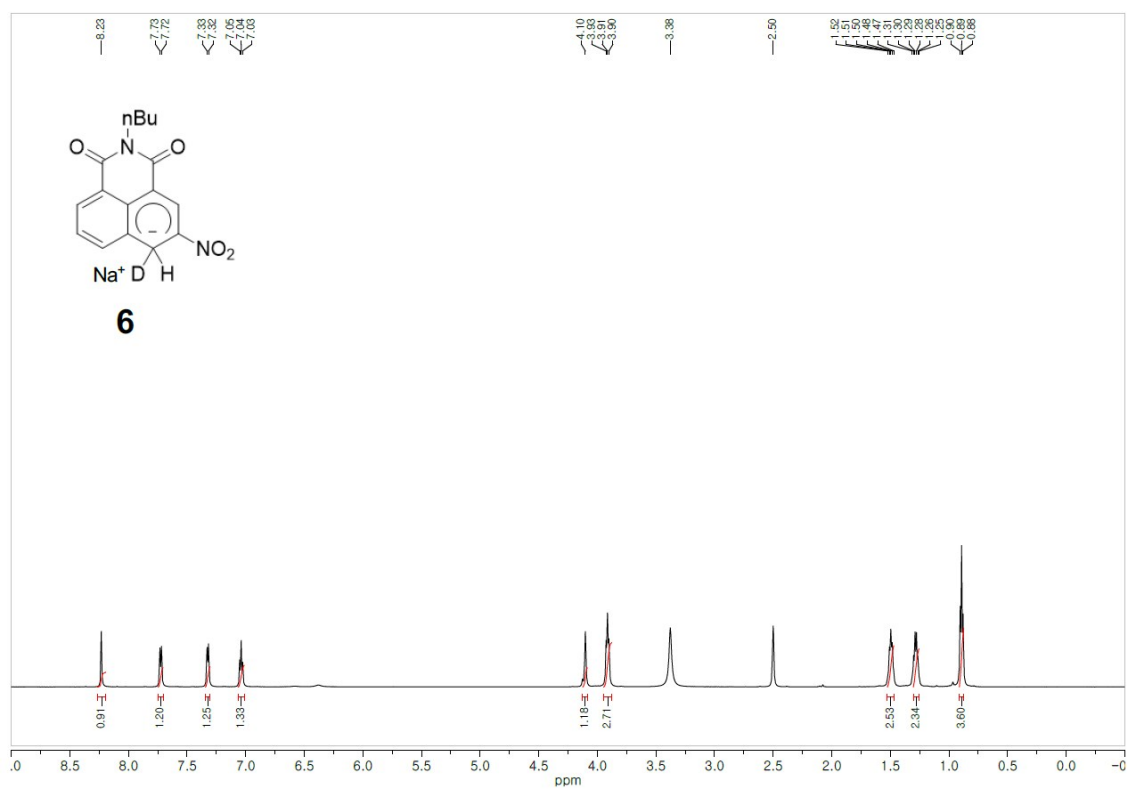


Fig. S7. High-resolution ESI mass spectrum of hydride-Meisenheimer adduct **5** obtained from **BP-3N** after treatment with sodium borohydride in acetonitrile.

^1H NMR



^{13}C NMR

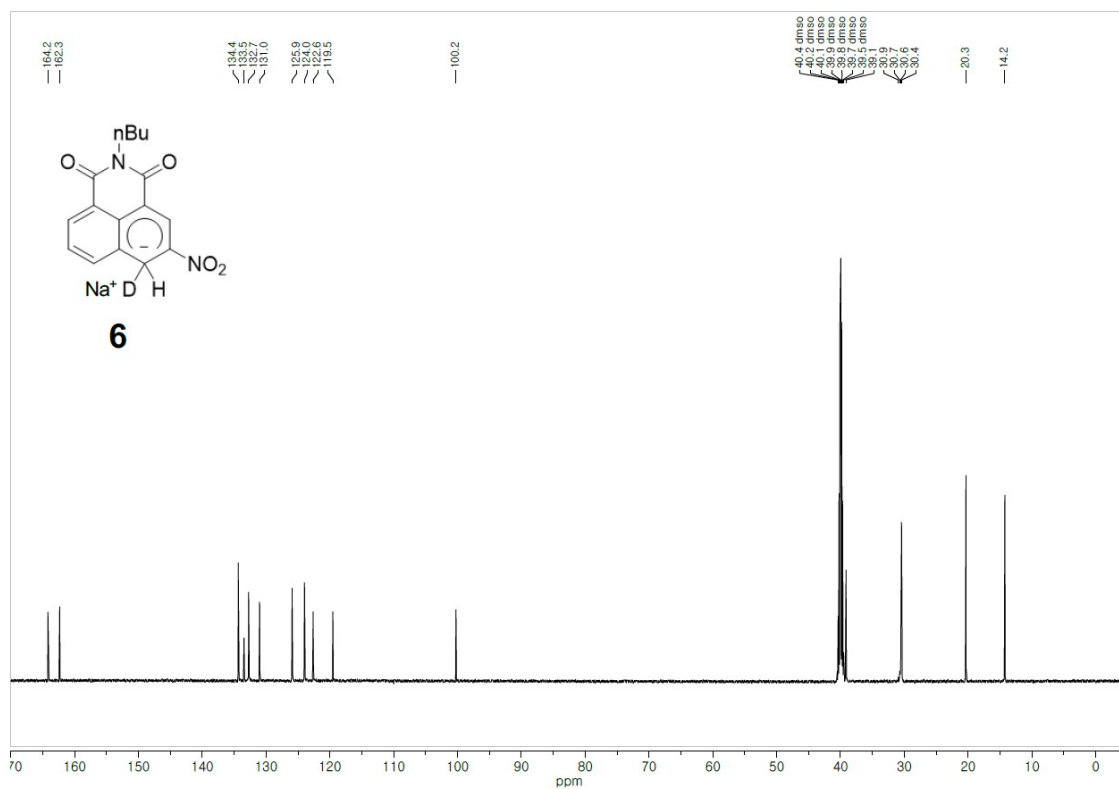


Fig. S8. ^1H and ^{13}C NMR spectra of deuteride-Meisenheimer adduct **6** in $\text{DMSO-}d_6$.

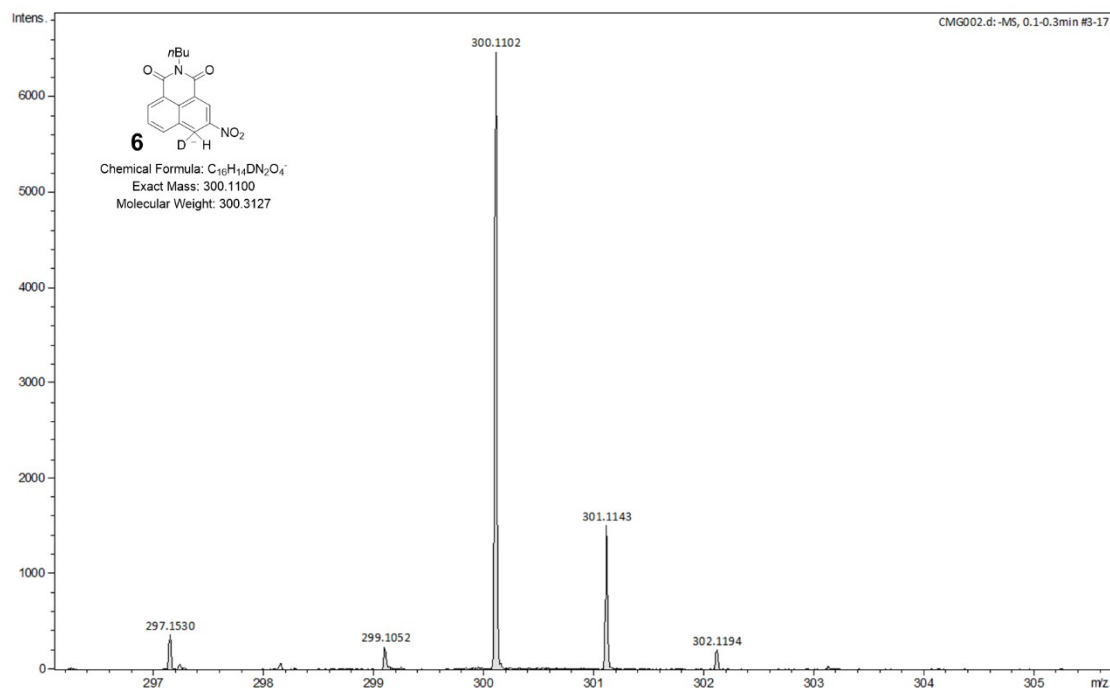


Fig. S9. High-resolution ESI mass spectrum of deuteride-Meisenheimer adduct **6** obtained from **BP-3N** after treatment with $NaBD_4$.

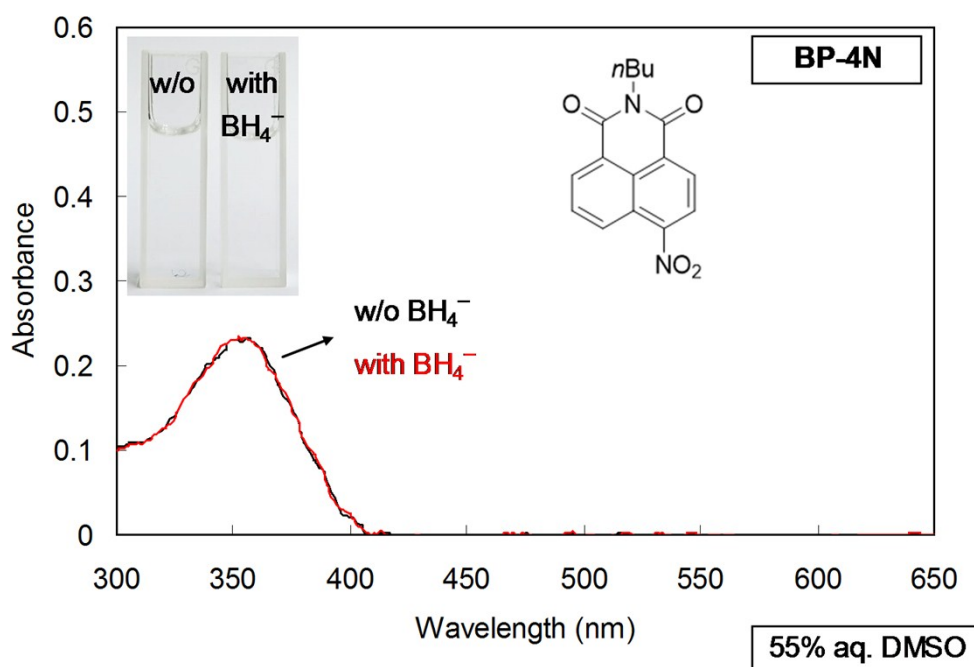


Fig. S10. UV-vis spectra of **BP-4N** in the presence and absence of borohydride in aqueous DMSO. $[BP-4N] = 2.0 \times 10^{-5}$ M, $[NaBH_4] = 4.0 \times 10^{-4}$ M in 55:45 (v/v) mixture of Na_2HPO_4 -NaOH buffer (pH 11.0, final concentration = 10 mM) and DMSO.

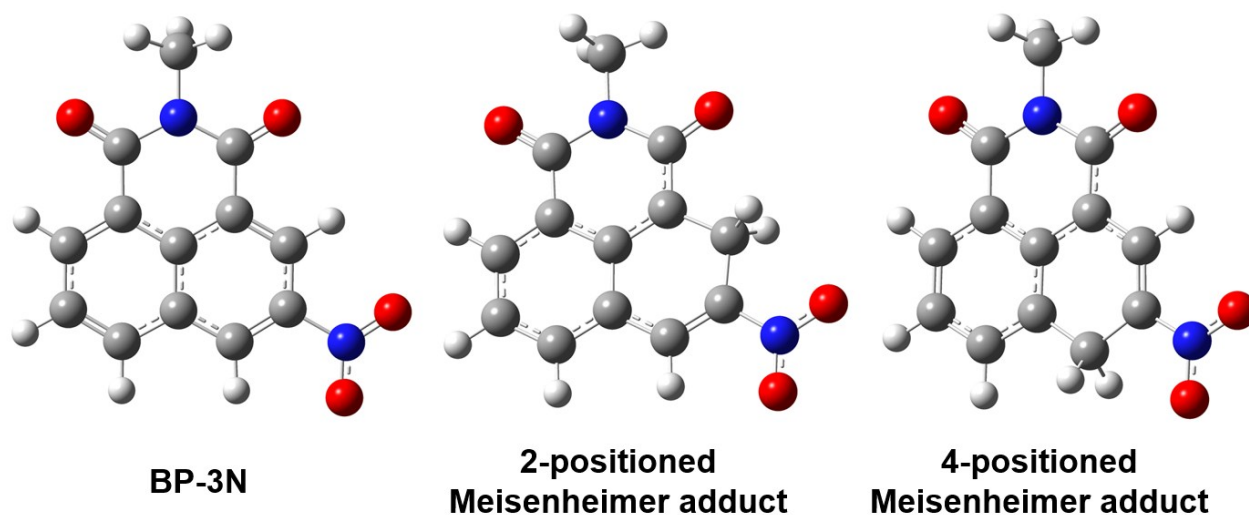


Fig. S11. Optimized structures of **BP-3N**, and 2-positioned-, and 4-positioned-Meisenheimer adducts.

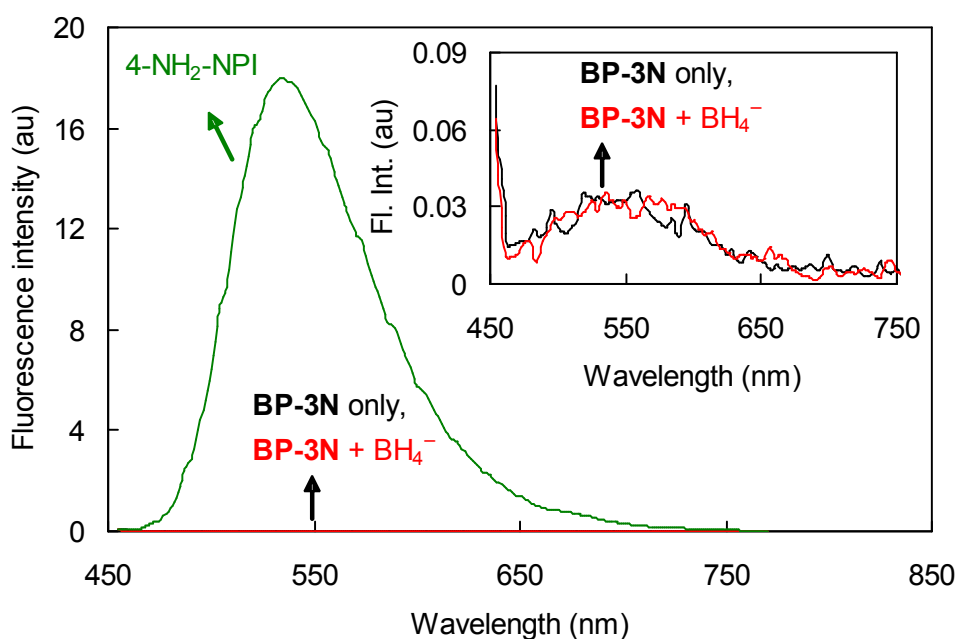


Fig. S12. Fluorescence spectra of **BP-3N** in the presence and absence of borohydride, and *n*-butyl-4-aminonaphthalimide (4-NH₂-NPI) as the fluorescence reference. [**BP-3N**] = 1.0×10^{-5} M, [NaBH₄] = 2.0×10^{-4} M, [4-NH₂-NPI] = 1.0×10^{-5} M in 55:45 (v/v) mixture of Na₂HPO₄-NaOH buffer (pH 11.0, final concentration = 10 mM) and DMSO. λ_{ex} = 450 nm.

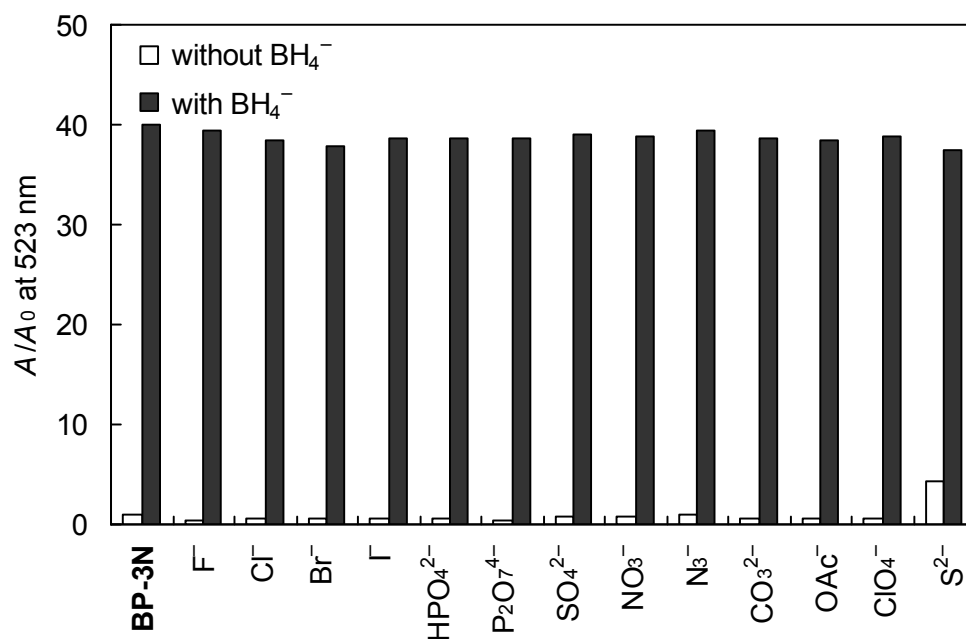


Fig. S13. Selective borohydride signaling of **BP-3N** over common anions as expressed by the absorbance ratio (A/A_0) at 523 nm. $[\text{BP-3N}] = 2.0 \times 10^{-5} \text{ M}$, $[\text{NaBH}_4] = [\text{A}^{n-}] = 4.0 \times 10^{-4} \text{ M}$ in 55:45 (v/v) mixture of Na_2HPO_4 -NaOH buffer (pH 11.0, final concentration = 10 mM) and DMSO solution.

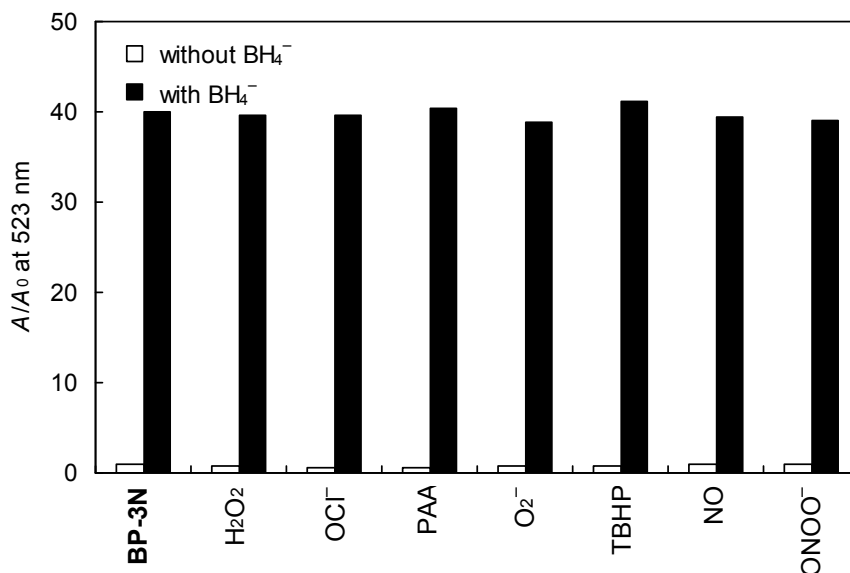


Fig. S14. Selective borohydride signaling of **BP-3N** over common reactive oxygen and nitrogen species (ROS/RNS) as expressed by the absorbance ratio (A/A_0) at 523 nm. $[\text{BP-3N}] = 2.0 \times 10^{-5} \text{ M}$, $[\text{NaBH}_4] = [\text{ROS/RNS}] = 4.0 \times 10^{-4} \text{ M}$ in 55:45 (v/v) mixture of Na_2HPO_4 -NaOH buffer (pH 11.0, final concentration = 10 mM) and DMSO solution. PAA = peracetic acid, TBHP = *tert*-butyl hydroperoxide.

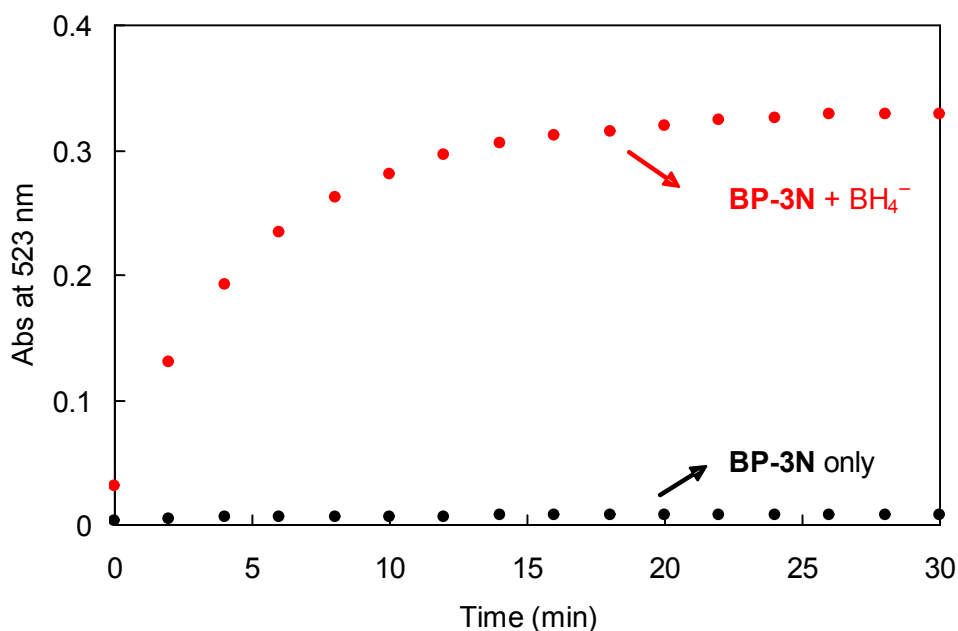


Fig. S15. The time-course plot of the absorbance change of **BP-3N** at 523 nm during reaction with borohydride. $[\text{BP-3N}] = 2.0 \times 10^{-5} \text{ M}$, $[\text{NaBH}_4] = 4.0 \times 10^{-4} \text{ M}$ in 55:45 (v/v) mixture of Na_2HPO_4 - NaOH buffer (pH 11.0, final concentration = 10 mM) and DMSO.

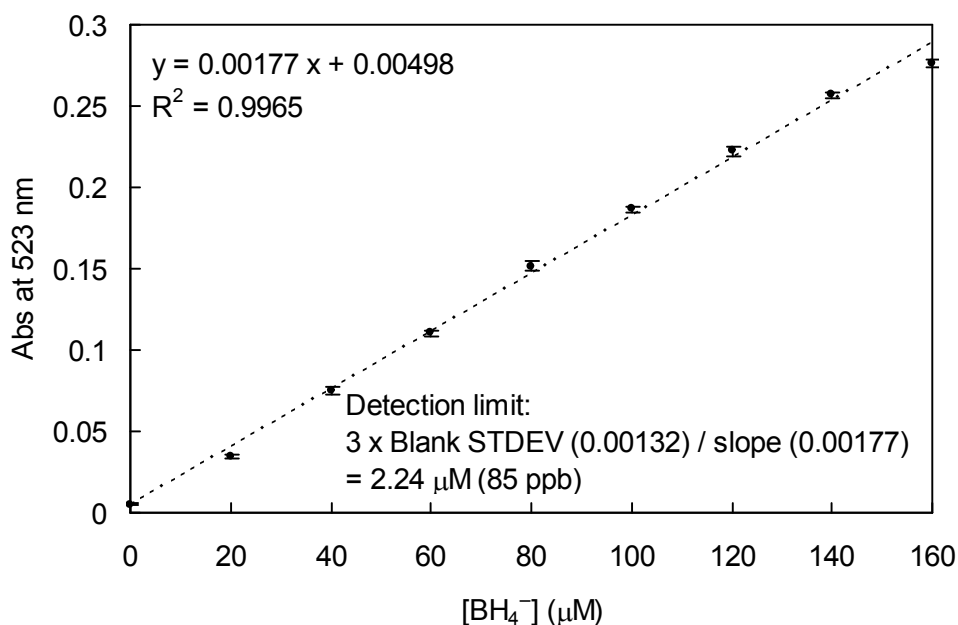


Fig. S16. Concentration dependence of borohydride signaling by **BP-3N**. $[\text{BP-3N}] = 2.0 \times 10^{-5} \text{ M}$, $[\text{NaBH}_4] = 0\text{--}1.6 \times 10^{-4} \text{ M}$ in 55:45 (v/v) mixture of Na_2HPO_4 - NaOH buffer (pH 11.0, final concentration = 10 mM) and DMSO. Error bars were obtained from three independent experiments.

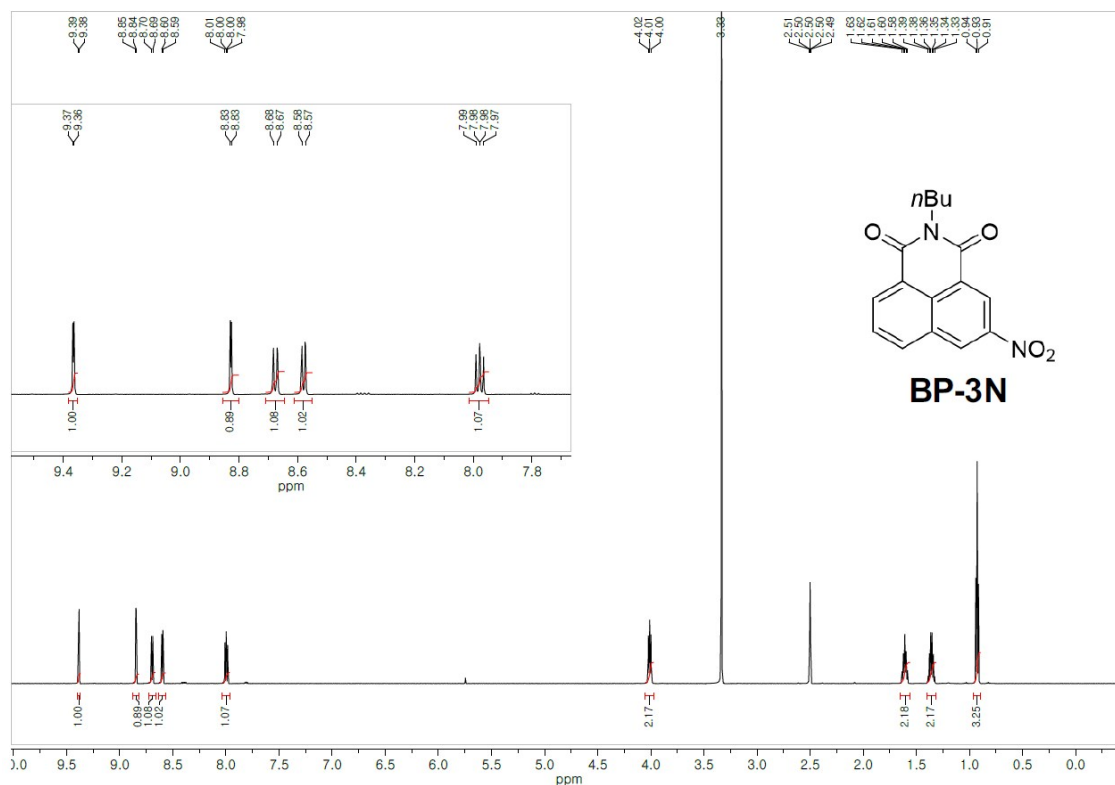


Fig. S17. ¹H NMR spectrum of **BP-3N** in DMSO-*d*₆ (600 MHz).

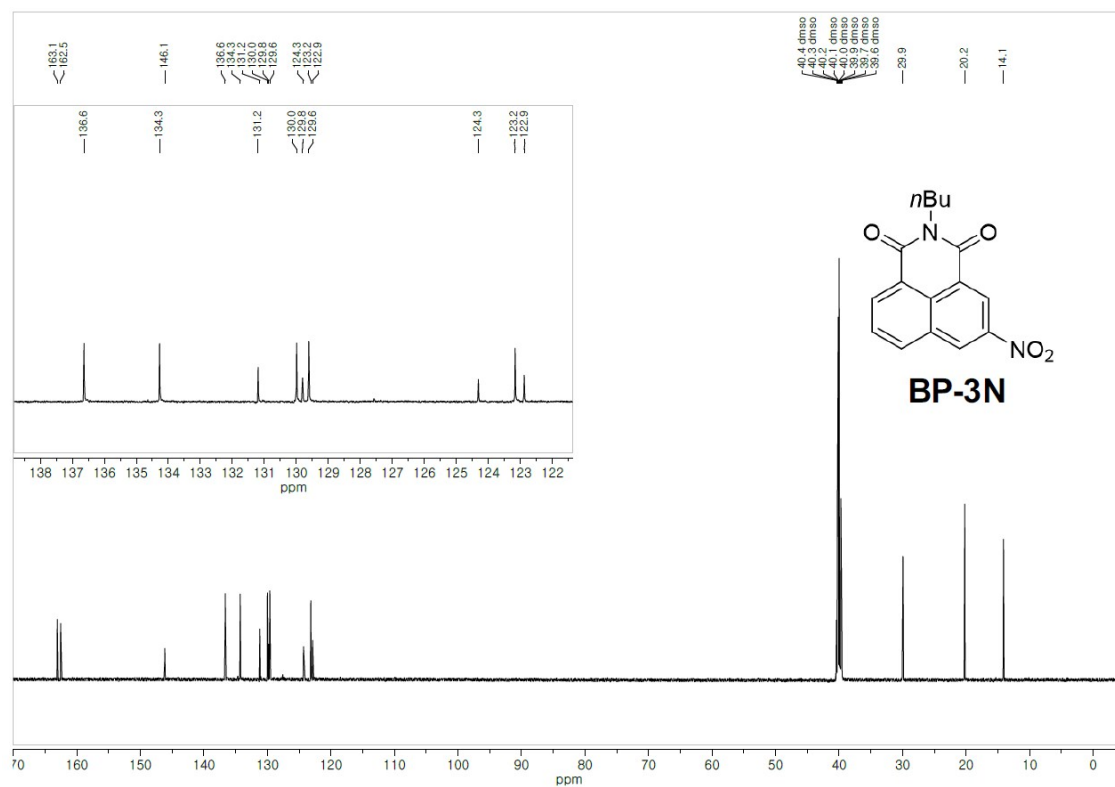


Fig. S18. ¹³C NMR spectrum of **BP-3N** in DMSO-*d*₆ (150 MHz).

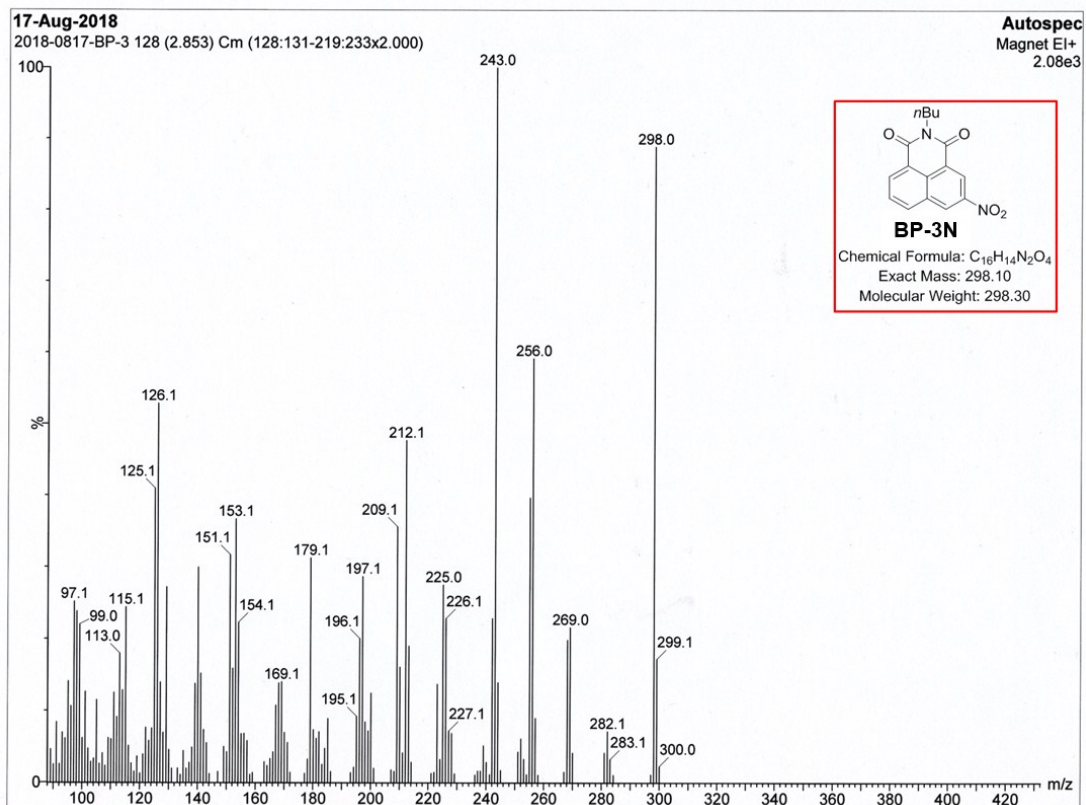


Fig. S19. Electron ionization mass spectrum (direct insertion probe) of BP-3N.

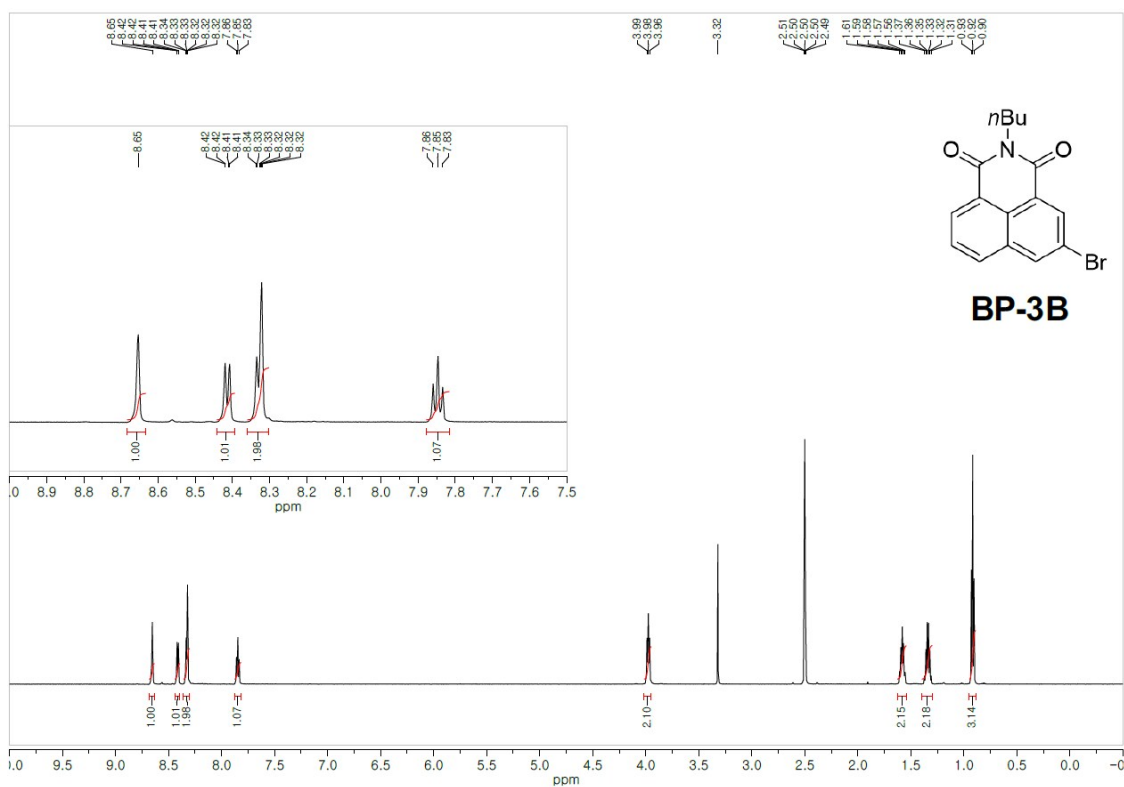


Fig. S20. ¹H NMR spectrum of BP-3B in DMSO-d₆ (600 MHz).

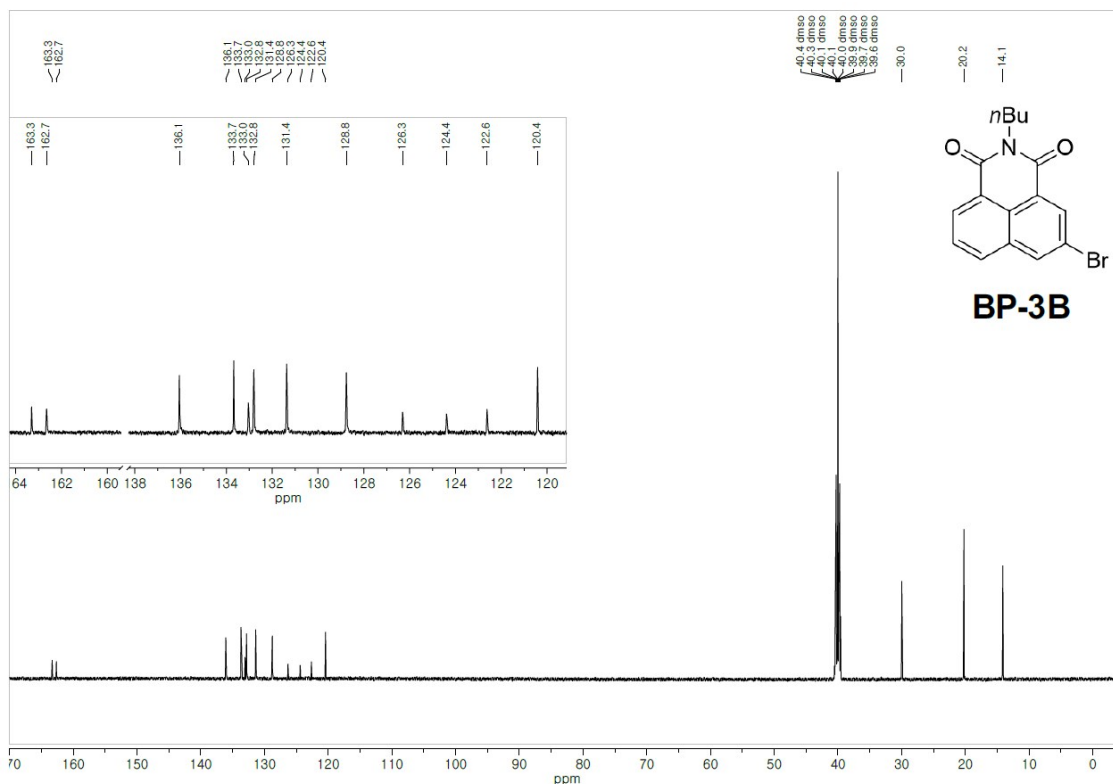


Fig. S21. ¹³C NMR spectrum of **BP-3B** in DMSO-*d*₆ (150 MHz).

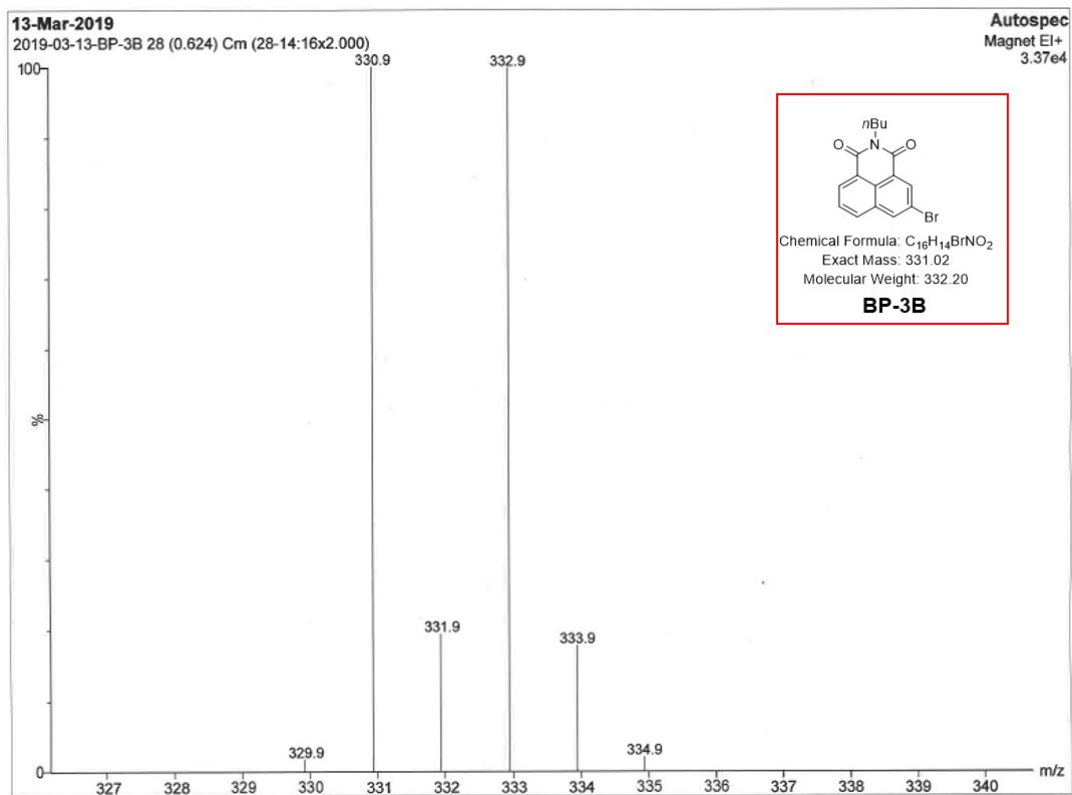


Fig. S22. Electron ionization mass spectrum (direct insertion probe) of **BP-3B**.

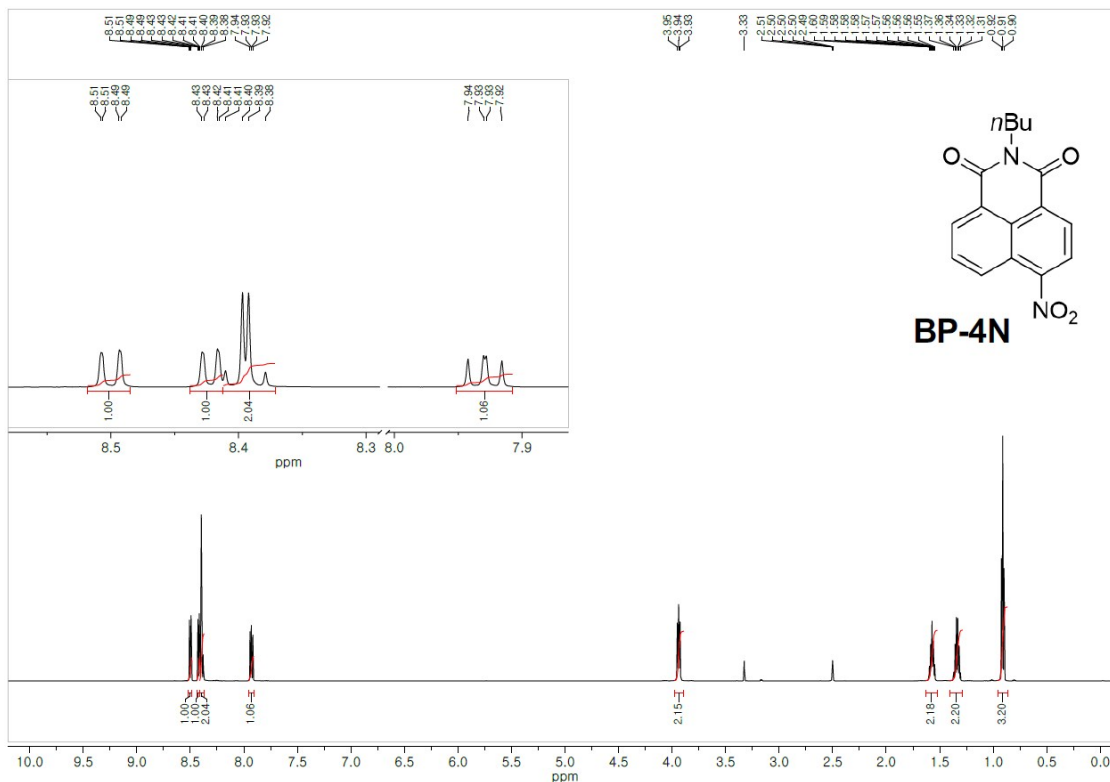


Fig. S23. ^1H NMR spectrum of **BP-4N** in $\text{DMSO-}d_6$ (600 MHz).

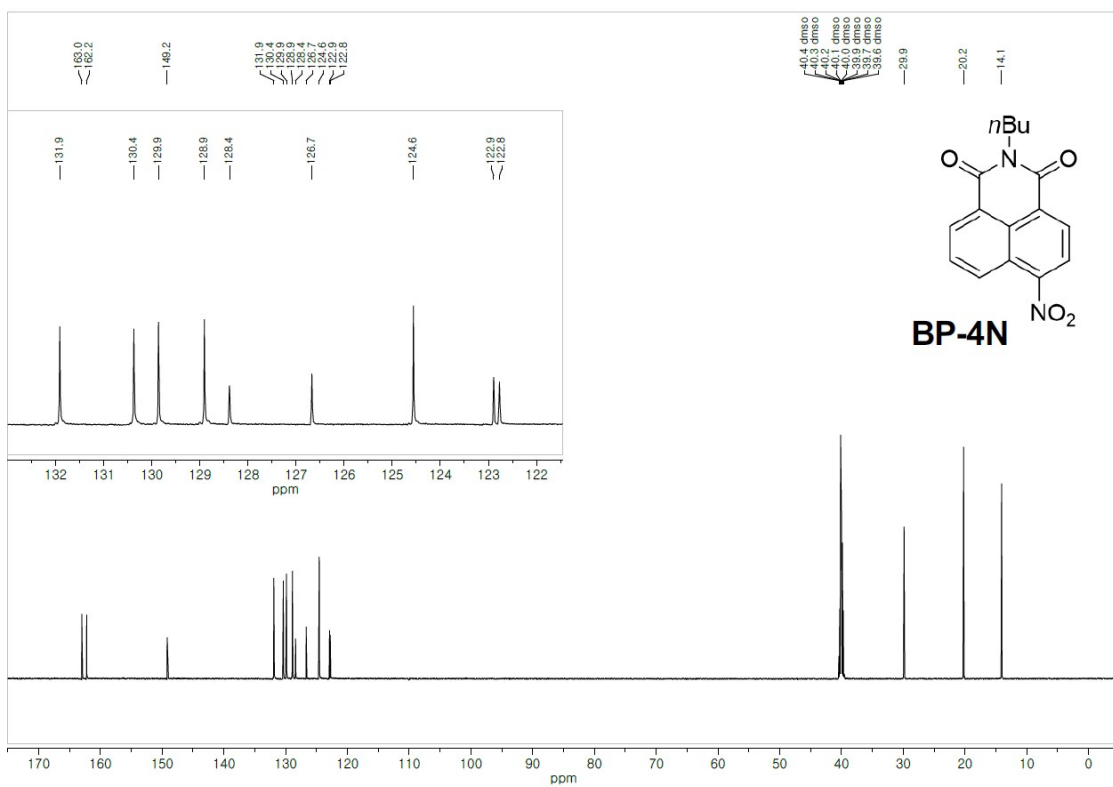


Fig. S24. ^{13}C NMR spectrum of **BP-4N** in $\text{DMSO-}d_6$ (150 MHz).

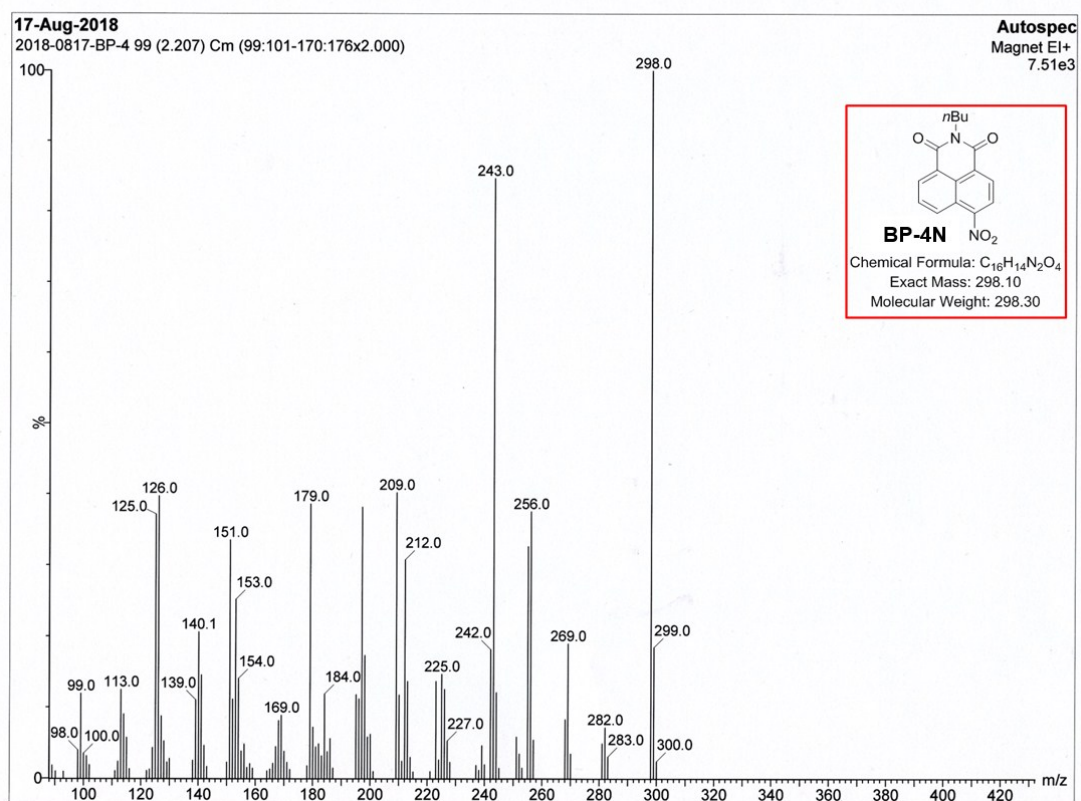


Fig. S25. Electron ionization mass spectrum (direct insertion probe) of BP-4N.

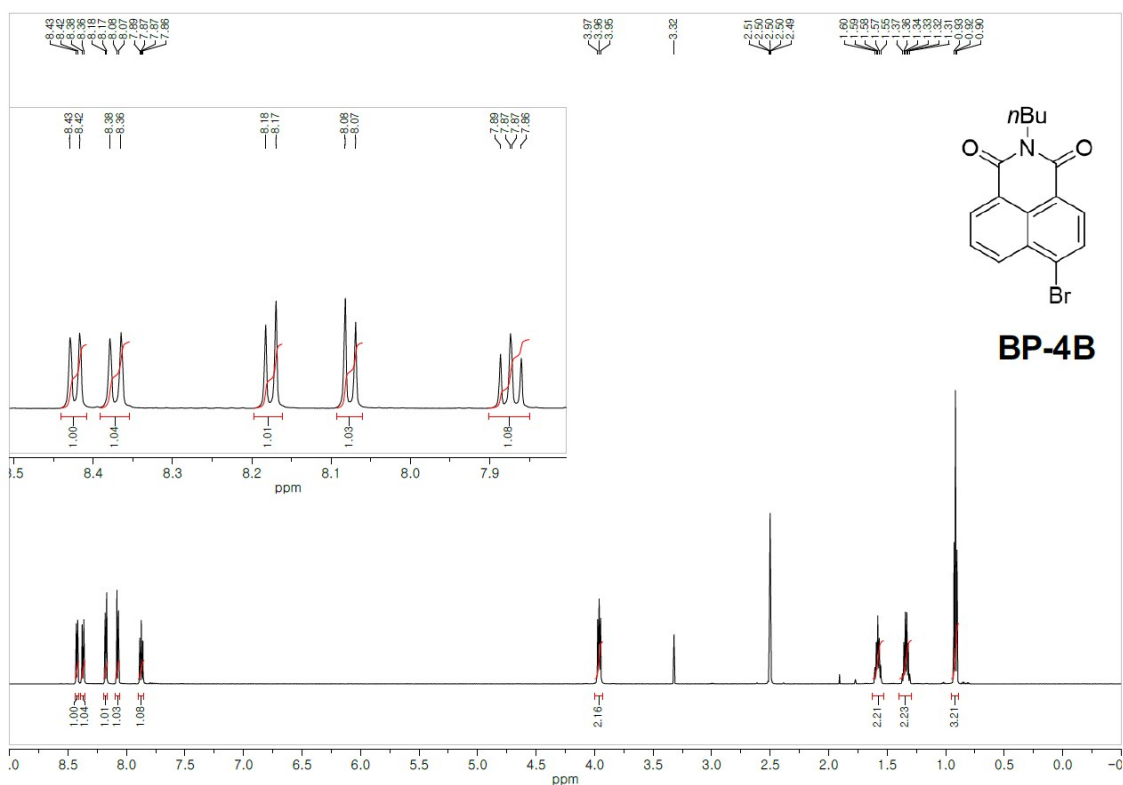


Fig. S26. ^1H NMR spectrum of BP-4B in $\text{DMSO-}d_6$ (600 MHz).

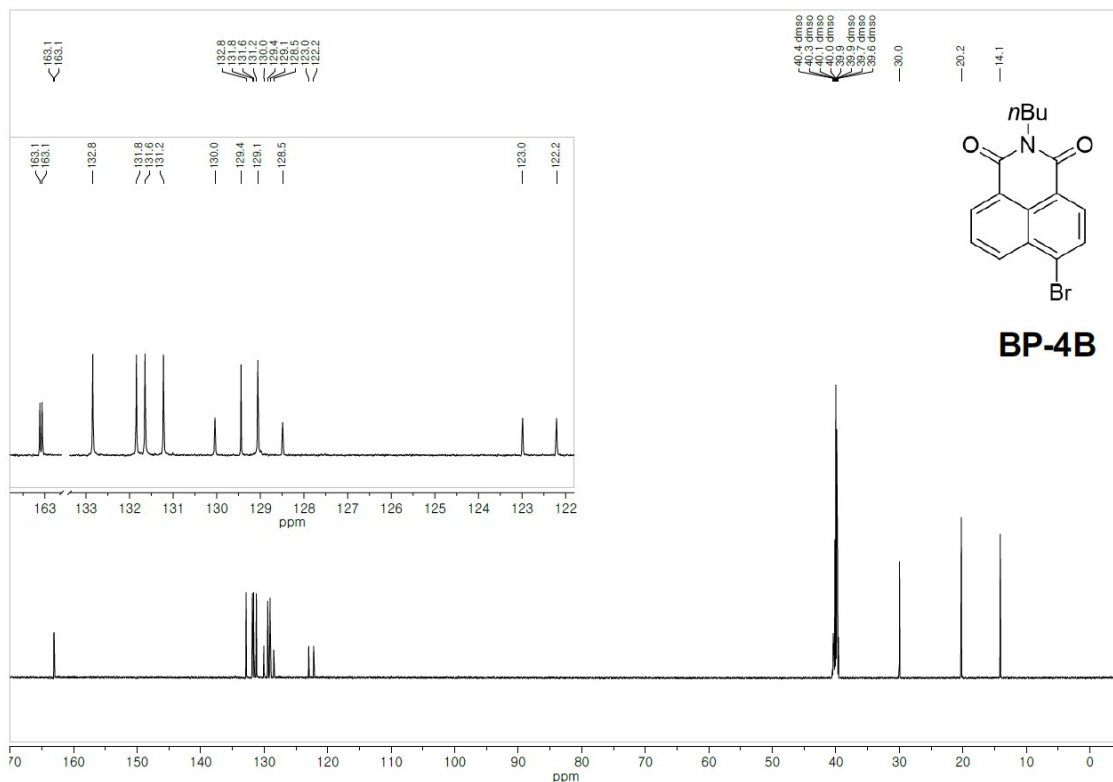


Fig. S27. ^{13}C NMR spectrum of **BP-4B** in $\text{DMSO-}d_6$ (150 MHz).

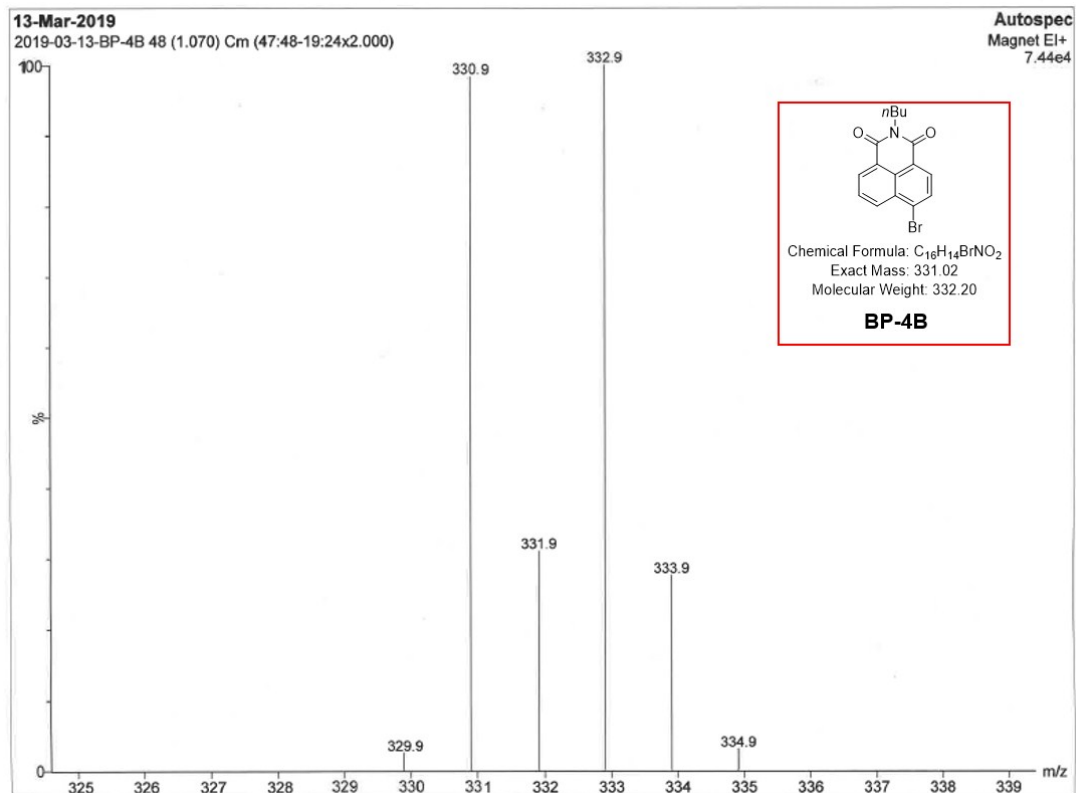


Fig. S28. Electron ionization mass spectrum (direct insertion probe) of **BP-4B**.

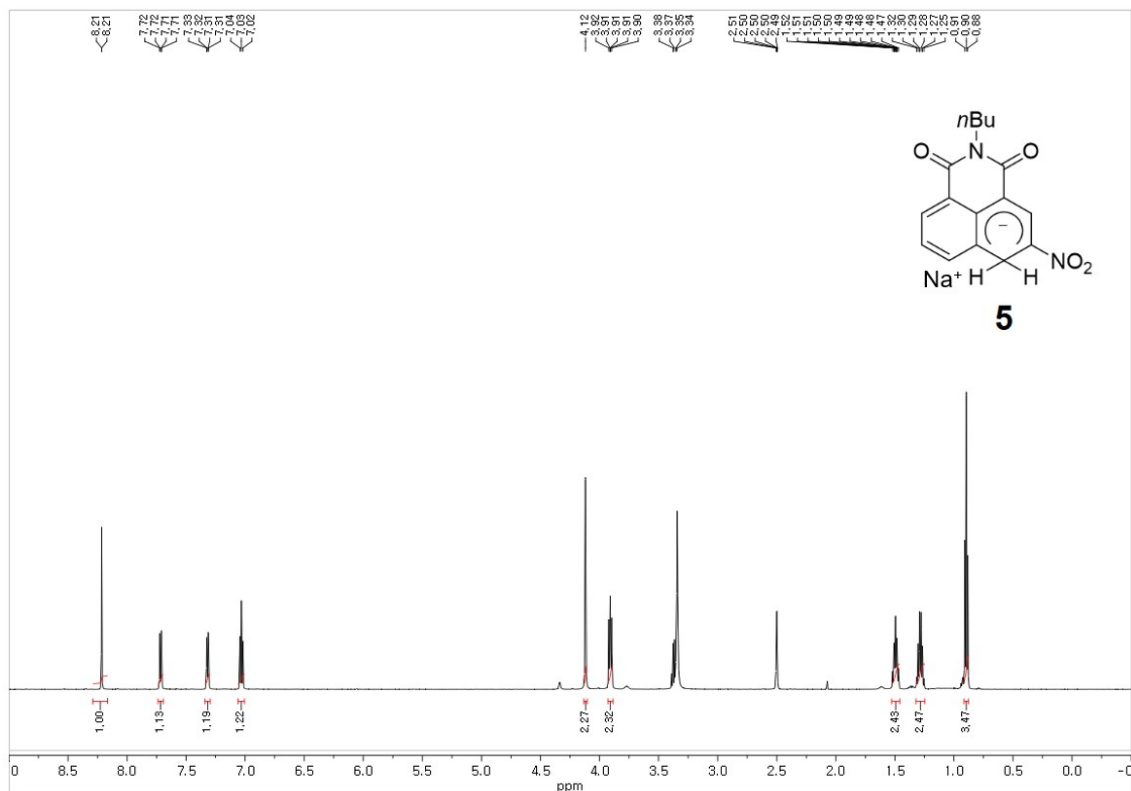


Fig. S29. ¹H NMR spectrum of hydride-Meisenheimer adduct **5** in DMSO-*d*₆ (600 MHz).

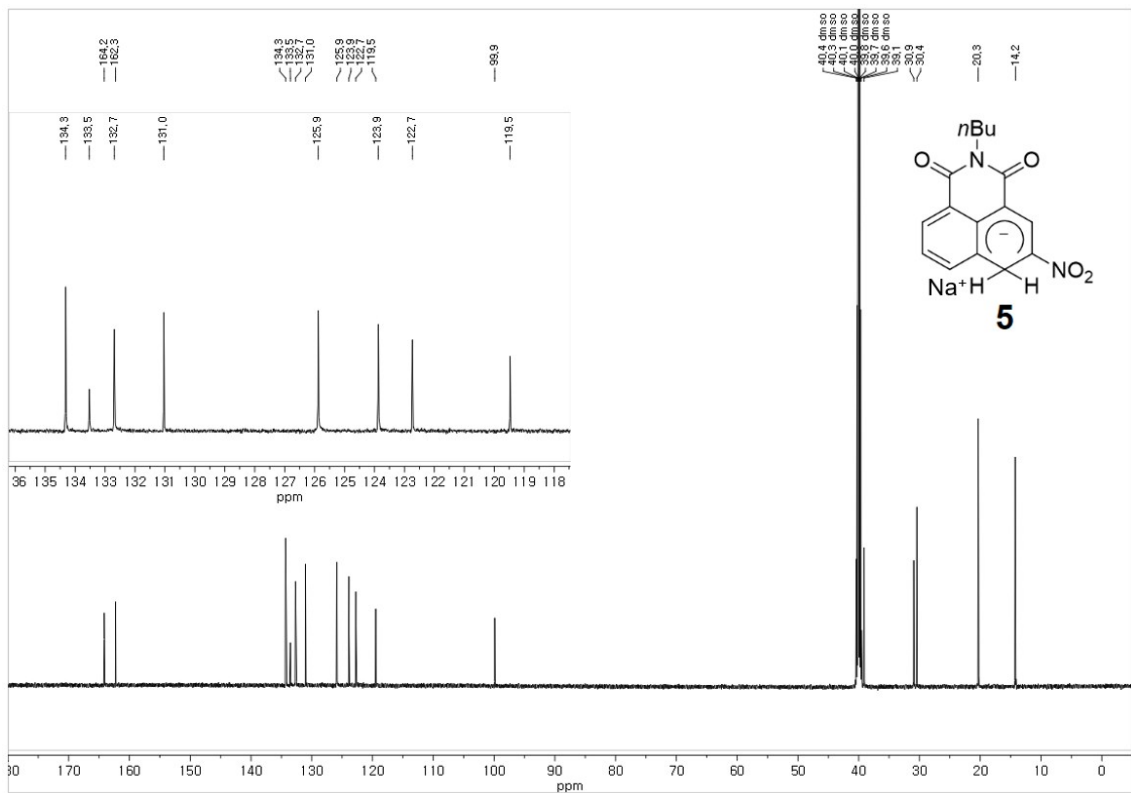


Fig. S30. ¹³C NMR spectrum of hydride-Meisenheimer adduct **5** in DMSO-*d*₆ (150 MHz).

References

- (S1) D. A. Lytle, E. H. Jensen and W. A. Struck, *Anal. Chem.* 1952, **24**, 1843–1844.
- (S2) E. R. Triboni, P. B. Filho, R. G. de Souza Berlinck and M. J. Politi, *Synth. Commun.*, 2004, **34**, 1989–1999.
- (S3) J. Wu, R. Huang, C. Wang, W. Liu, J. Wang, X. Weng, T. Tian and X. Zhou, *Org. Biomol. Chem.*, 2013, **11**, 580–585.
- (S4) J. Tyman, *Synth. Commun.*, 1989, **19**, 179–188.
- (S5) J. Wang, *Dyes Pigment.*, 2007, **74**, 103–107.
- (S6) D. D. Perin and B. Dempsey, in *Buffers for pH and Metal Ion Control*, Chapman and Hall Ltd, London, 1979, p 151.
- (S7) Gaussian 09, Revision C.01, M. J. Frisch, G. W. Trucks, H. B. Schlegel, et al. Gaussian, Inc., Wallingford CT, 2010.
- (S8) J. A. Krynitsky, J. E. Johnson and H. W. Carhart, *Anal. Chem.*, 1948, **20**, 311–312.
- (S9) D. M. F. Santos and C. A. C. Sequeira, *Int. J. Hydrogen Energy*, 2010, **35**, 9851–9861.
- (S10) S. W. Charkin, *Anal. Chem.*, 1953, **25**, 831–832.
- (S11) I. E. Lichtenstein and J. S. Mras, *J. Frankl. Inst.-Eng. Appl. Math.*, 1966, **281**, 481–485.
- (S12) H. C. Brown and A. C. Boyd, Jr., *Anal. Chem.*, 1955, **27**, 156–157.
- (S13) M. V. Mirkin and A. J. Bard, *Anal. Chem.*, 1991, **63**, 532–533.
- (S14) S. Botasini and E. Méndez, *J. Power Sources*, 2012, **197**, 218–223.
- (S15) K. T. Møller, A. S. Fogh, M. Paskevicius, J. Skibsted and T. R. Jensen, *Phys. Chem. Chem. Phys.*, 2016, **18**, 27545–27553.
- (S16) E. L. Gyenge and C. W. Oloman, *J. Applied Electrochem.*, 1998, **28**, 1147–1151.
- (S17) N. Y. Kim, J. H. Beak and S.-K. Chang, *Tetrahedron Lett.*, 2019, **60**, 59–62.
- (S18) D. A. Werner, C. C. Huang and D. Aminoff, *Anal. Biochem.*, 1973, **54**, 554–560.
- (S19) B. Elamin and G. E. Means, *Anal. Chim. Acta*, 1979, **107**, 405–409.
- (S20) C. N. Rudie and P. R. Demko, *J. Am. Oil Chem. Soc.*, 1979, **56**, 520–521.